Journal of Computational Physics **173,** 116–148 (2001)
doi:10.1006/jcph.2001.6854, available online at http://www.idealibrary.com on IDEAL®

Geometric Integrators for the Nonlinear Schrödinger Equation

A. L. Islas,* D. A. Karpeev,† and C. M. Schober‡

*Department of Mathematics and Statistics, Old Dominion University, Norfolk, Virginia 23529; †Department of Computer Science, Old Dominion University, Norfolk, Virginia 23529; and ‡Department of Mathematics and Statistics, Old Dominion University, Norfolk, Virginia 23529
E-mail: islas@math.odu.edu; karpeev@cs.odu.edu; cschober@lions.odu.edu

Received August 21, 2000; revised June 8, 2001

Recently an interesting new class of PDE integrators, multisymplectic schemes, has been introduced for solving systems possessing a certain multisymplectic structure. Some of the characteristic features of the method are its local nature (independent of boundary conditions) and an equal treatment of spatial and temporal variables. The nonlinear Schrödinger equation (NLS) has a multisymplectic formulation, and in this paper we discuss the performance of both symplectic and multisymplectic integrators for the NLS. In the numerical experiments, the multisymplectic concatenated midpoint scheme (a centered cell discretization) is shown to preserve the local conservation laws extremely well over long times and to preserve global invariants such as the norm and momentum within roundoff. On the other hand, an integrable Hamiltonian semi-discretization of NLS from Ablowitz and Ladik (AL) possesses a full set of global conservation laws and a noncanonical symplectic structure. We generalize the generating function technique to develop symplectic integrators of arbitrary order for a general class of noncanonical systems carrying a symplectic structure of the AL type. Another approach examined in the paper is the introduction of transformations to reduce the AL system to either (1) separable form or (2) canonical form and then apply standard schemes in the new coordinates. All of the discretizations are tested numerically using initial data for spatially periodic multiphase solutions. The performance of the schemes as well as interrelations among various geometric features are discussed.

Key Words: symplectic integrators; multisymplectic integrators; nonlinear Schrödinger equation; nonlinear wave equations.

1. INTRODUCTION

Numerical schemes which preserve the geometric features of the system under study have become very popular. In particular, symplectic schemes which are designed to preserve

0021-9991/01 $35.00

the symplectic structure of canonical Hamiltonian ODEs have demonstrated a remarkable ability to preserve the phase space geometry for very long times. In the low-dimensional case, symplectic discretizations conserve the integrals of motion of the original system extremely well. However, systems with a noncanonical symplectic structure have remained largely unexamined, with a few exceptions such as the linear *Lie–Poisson* case and the Ablowitz–Ladik discrete nonlinear Schrodinger equation [22]. The reason for this is partly the fact that any nondegenerate symplectic structure can be reduced to the canonical one via a suitable local coordinate transformation (Darboux's Theorem) [5]. The numerical practicality of such transformations for integration of noncanonical systems remains an open question. While symplectic discretizations that directly preserve the noncanonical structure can be derived (as shown in Section 4), they typically are highly nonlinear and implicit and thus computationally expensive in comparison to traditional schemes.

In a broader context, an important question which is actively under study is how to appropriately generalize symplectic integrators to a Hamiltonian PDE framework, i.e. what are the relevant geometric features for a PDE integrator to preserve. One long standing approach to this problem (which has met with varying degrees of success) has been to introduce a Hamiltonian semi-discretization of the PDE using, for example, spectral methods or finite differencing and then applying a symplectic scheme to integrate the semi-discrete system in time; see e.g. [4, 10, 12, 14, 16, 23]. The resulting numerical schemes preserve the symplectic structure of the semi-discretization but as the level of discretization is refined or the dimension of the system is increased, the advantage obtained using the symplectic integrator can occur only on a long enough timescale (see the numerical experiments in Section 5.1). Another problem with this method is its nonlocality as the system is defined on a particular phase space which enforces a specific type of boundary condition. Yet often local features of solutions or even existence and properties of a particular class of solutions (e.g., spatial and/or temporal (quasi)periodicity) are of interest.

An alternate generalization to the PDE framework involves a local concept of symplecticity and the introduction of "multisymplectic integrators" [6, 7, 15]. Bridges and Reich [7] consider PDEs with the following geometrical structure (for convenience we restrict to the "$1+1$" case of one spatial and one temporal dimensions): Let $\boldsymbol{M}$ and $\boldsymbol{K}$ be *any* skew–symmetric matrices on $\mathbb{R}^{n\times n}(n \geq 3)$ and let $S:\mathbb{R}^n \mapsto \mathbb{R}$ be *any* smooth function. Then, a system of the following form

$$\boldsymbol{M}\boldsymbol{z}_t + \boldsymbol{K}\boldsymbol{z}_x = \boldsymbol{\nabla}_z S(\boldsymbol{z}), \quad \boldsymbol{z} \in \mathbb{R}^n, \tag{1}$$

(the gradient $\boldsymbol{\nabla}_{\boldsymbol{z}}$ is defined with respect to the standard inner product on $\mathbb{R}^n$) is called a *Hamiltonian system on a multisymplectic structure* or, in brief, a multisymplectic PDE.

The term multisymplectic is applied to system (1) in the following sense. Associated with $\boldsymbol{M}$ and $\boldsymbol{K}$ are the two forms

$$\omega(U,V) = \langle \boldsymbol{M}U, V\rangle = V^T\boldsymbol{M}U \quad \text{and} \quad \kappa(U,V) = \langle \boldsymbol{K}U, V\rangle = V^T\boldsymbol{K}U, \quad U, V \in \mathbb{R}^n, \tag{2}$$

where ω defines a symplectic structure on $\mathbb{R}^m$ ($m = \operatorname{rank}\boldsymbol{M} \leq n$) associated with the time direction, and κ defines a symplectic structure on $\mathbb{R}^k$ ($k = \operatorname{rank}\boldsymbol{K} \leq n$) associated with the x-direction. An important aspect of a multisymplectic structure is that it admits a multisymplectic conservation law. Specifically, let $U, V \in \mathbb{R}^n$ be any two solutions of the

variational equation associated with (1),

$$\boldsymbol{M}d\boldsymbol{z}_t + \boldsymbol{K}d\boldsymbol{z}_x = \boldsymbol{D}_{\boldsymbol{zz}}\boldsymbol{S}(\boldsymbol{z})d\boldsymbol{z}. \tag{3}$$

Then

$$\begin{aligned} \partial_t \omega &= \langle \boldsymbol{M}U_t, V\rangle + \langle \boldsymbol{M}U, V_t\rangle \\ \partial_x \kappa &= \langle \boldsymbol{K}U_x, V\rangle + \langle \boldsymbol{K}U, V_x\rangle \end{aligned} \tag{4}$$

and noting that $\boldsymbol{D}_{\boldsymbol{zz}}\boldsymbol{S}(\boldsymbol{z})$ is a symmetric matrix, one obtains the multisymplectic conservation law

$$\begin{aligned} \partial_t \omega + \partial_x \kappa &= \langle \boldsymbol{M}U_t + \boldsymbol{K}U_x, V\rangle - \langle U, \boldsymbol{M}V_t + \mathbf{K}V_x\rangle \\ &= \langle \boldsymbol{D}_{\boldsymbol{zz}}\boldsymbol{S}(\boldsymbol{z})U, V - \langle U, \boldsymbol{D}_{\boldsymbol{zz}}\boldsymbol{S}(\boldsymbol{z})V\rangle \\ &= 0. \end{aligned} \tag{5}$$

Using wedge product notation, (5) is equivalent to

$$\partial_t[d\boldsymbol{z} \wedge \boldsymbol{M}d\boldsymbol{z}] + \partial_x[d\boldsymbol{z} \wedge \boldsymbol{K}d\boldsymbol{z}] = 0. \tag{6}$$

Multisymplectic integrators are approximations to (1) which conserve a discretization of the multisymplectic conservation law (5). Many analogies exist between symplectic and multisymplectic structures; likewise between the properties of symplectic and multisymplectic integrators. Conservation of multisymplecticity (5) is analogous to preservation of the two-form, $\omega_t = 0$, for Hamiltonian ODEs. In fact, let

$$\boldsymbol{z} = (p_1, \ldots, p_N, q_1, \ldots, q_N), \quad \boldsymbol{M} \equiv \boldsymbol{J} = \begin{pmatrix} \mathbf{0} & -\mathbf{I}_N \\ \mathbf{I}_N & \mathbf{0} \end{pmatrix},$$

where all p_j, q_j are spatially independent, then $\partial_x d\boldsymbol{z} \equiv 0$ leads to $\partial_x \kappa = \partial_x[d\boldsymbol{z} \wedge \boldsymbol{K}d\boldsymbol{z}] \equiv 0$ and (6) reduces to

$$\omega_t = \partial[d\boldsymbol{z} \wedge \boldsymbol{J}d\boldsymbol{z}] = d\boldsymbol{p} \wedge d\boldsymbol{q} = 0,$$

recovering the familiar notion of preservation of the canonical symplectic structure by the phase flow. As symplectic integrators are discretizations preserving the two-form ω, multisymplectic integrators are approximations to (1) which also conserve a discretization of the multisymplectic conservation law (5). Similarly, just as symplectic schemes conserve the Hamiltonian extremely well over very long times, multisymplectic schemes conserve the related energy and momentum conservation laws very well (see the results in Section 5.1).

Many integrable Hamiltonian PDEs (e.g., the sine-Gordon (SG) and NLS equations) can be expressed in a multisymplectic form. Earlier numerical studies of the NLS and SG equations [2, 4, 18] showed that the manner in which the PDE is spatially discretized is of prime importance for accurate resolution of the qualitative features of the system. For example, for initial values in the vicinity of homoclinic orbits, standard Hamiltonian discretizations may completely break down and generate spurious temporally chaotic solutions [18]. In this

paper, we examine the advantages of using geometric integrators to preserve the essential geometric features of the nonlinear Schrödinger (NLS) system

$$\begin{aligned} iq_t + q_{xx} + 2q^2 p &= 0 \\ -ip_t + p_{xx} + 2p^2 q &= 0 \end{aligned} \tag{7}$$

when periodic boundary conditions $(q(x + L, t),\ p(x + L, t)) = (q(x, t),\ p(x, t))$ are imposed. Specifically, for the integrable case $(p = q^*)$ we consider multisymplectic schemes as well as integrable spatial discretizations with symplectic integrators in time-integrable symplectic schemes.

To derive discretizations preserving the multisymplectic structure of NLS we employ the Gauss–Legendre (G–L) family of schemes, which is suitable for integration of nonlinear wave equations. These integrators were introduced and carefully implemented for the sine-Gordon equation in [20]. Here we apply the second-order member of the family to NLS and examine the preservation of the local and global conservation laws. As the numerical experiments demonstrate, multisymplectic methods have much to offer. For instance, the local and global energy are preserved far better than expected given the order of the scheme. In addition, the scheme is faster than other second-order geometric integrators examined in the paper and preserves the conjugacy relation between complex coordinates $(p = q^*)$.

Perhaps even more important than the multisymplectic structure is the integrable structure associated with NLS, so it is natural to consider discretizations preserving it. An interesting feature of the NLS is that its integrable semi-discretization, the Ablowitz–Ladik (AL) system (Eq. (37)), possesses a highly nontrivial noncanonical symplectic structure, even though the continuous system is canonical. The most general approach for developing symplectic discretizations for noncanonical Hamiltonian systems is to use the generating function technique. This method has been used for canonical Hamiltonian systems by many authors (e.g., [8, 21]). In [22] we extended the technique to generate a second-order scheme for the AL system. Here the algorithm is generalized to develop symplectic integrators of arbitrary order for a general class of noncanonical systems carrying a symplectic structure of the AL type. We implement the second-order member of the resulting family and test it numerically. The experiments show however, that the conjugacy relation $(\mathrm{p} = \mathrm{q}^*)$ is not preserved by the discrete flow. In fact, enforcing it as a separate constraint results in degradation of preservation of the constants of motion.

An alternate approach to preserving the symplectic structure is to transform the system into a form for which standard symplectic integrators can be applied. We introduce two such transformations. One transformation yields a noncanonical Hamiltonian system for which splitting methods can be applied. The second transformation, a Darboux transformation, reduces the AL symplectic structure to canonical form. We initiate a comparison between the various symplectic schemes for the AL system in canonical and noncanical form. We stress the applicability and potential usefulness of the generating function approach for general noncanonical Hamiltonian systems. The numerical experiments indicate that the generating function scheme is more efficient than the standard symplectic schemes applied to the transformed systems. In fact, such transformations appear to introduce additional complexity into the form of the equations that poses difficulty even for an efficient algorithm such as the implicit midpoint scheme. This demonstrates the difficulties in finding an optimal transform and that it can be more efficient to integrate the AL system in its original noncanonical form.

The rest of the paper is organized as follows. The Hamiltonian and multisymplectic structure of NLS is developed in Section 2. Next, in Section 3, the multisymplectic centered cell discretization, which arises by concatenating two second-order members of the G–L family, is applied to the NLS and its properties are discussed. In particular we find that for the NLS the multisymplectic scheme is actually symplectic in time in the traditional sense (the details are provided in the Appendix). In Section 4 we present the AL integrable discretization of the NLS in canonical and noncanonical form and develop several symplectic schemes for the AL system. Numerical experiments and their results are discussed in Section 5, where we compare the performance of the various integrators. In Section 6 we conclude the paper with a brief discussion of the relative merits of the various geometric integrators.

2. Hamiltonian and Multisymplectic Structure of the NLS Equation

In modeling a variety of physically significant nonlinear phenomena, the condition $p = \pm q^*$ is frequently imposed in (7) and in this case the system reduces to the standard cubic nonlinear Schrödinger equation (NLS)

$$i\,\partial_t q + \partial_{xx} q + 2|q|^2 q = 0. \tag{8}$$

The NLS equation is a completely integrable system in the sense of the inverse scattering transform (IST) and can be written as an infinite dimensional Hamiltonian system on H^1_{per} when periodic boundary conditions, $q(x + L, t) = q(x, t)$, are imposed

$$\partial_t \begin{pmatrix} q^* \\ q \end{pmatrix} = \boldsymbol{J} \begin{pmatrix} \delta H/\delta q^* \\ \delta H/\delta q \end{pmatrix}, \tag{9}$$

with $\boldsymbol{J} = \left(\begin{smallmatrix} 0 & -1 \\ 1 & 0 \end{smallmatrix}\right)$ and Hamiltonian

$$H(q^*, q) = i \int_0^L (|q|^4 - |q_x|^2)\, dx. \tag{10}$$

The symplectic form for the NLS is given by

$$\omega = \int_0^L \begin{pmatrix} dp \\ dq \end{pmatrix}^T \boldsymbol{J}^{-1} \begin{pmatrix} dp \\ dq \end{pmatrix} dx = \int_0^L (dp \wedge dq)\, dx. \tag{11}$$

Alternately, the NLS can be viewed as a multisymplectic Hamiltonian PDE of type (1). Letting $q = a - ib$, the NLS can be rewritten as a pair of real-valued equations

$$\begin{aligned} \partial_t a &= \partial_{xx} b + 2(a^2 + b^2)b, \\ \partial_t b &= -\partial_{xx} a - 2(a^2 + b^2)a. \end{aligned} \tag{12}$$

Introducing the pair of conjugate momenta $v = a_x$, $w = b_x$, system (11) has a multisymplectic formulation [20]

$$\boldsymbol{M}\boldsymbol{z}_t + \boldsymbol{K}\boldsymbol{z}_x = \nabla_{\boldsymbol{z}} \boldsymbol{S}(\boldsymbol{z}), \tag{13}$$

with

$$\boldsymbol{M} = \begin{pmatrix} 0 & 1 & 0 & 0 \\ -1 & 0 & 0 & 0 \\ 0 & 0 & 0 & 0 \\ 0 & 0 & 0 & 0 \end{pmatrix}, \quad \boldsymbol{K} = \begin{pmatrix} 0 & 0 & -1 & 0 \\ 0 & 0 & 0 & -1 \\ 1 & 0 & 0 & 0 \\ 0 & 1 & 0 & 0 \end{pmatrix}, \quad \boldsymbol{z} = [a, b, v, w]^T$$

and Hamiltonian

$$\boldsymbol{S}(\boldsymbol{z}) = \frac{1}{2}(v^2 + w^2 + (a^2 + b^2)^2),$$

i.e.,

$$\begin{aligned} -\partial_t b - \partial_x v &= 2(a^2 + b^2)a, \\ \partial_t a - \partial_x w &= 2(a^2 + b^2)b, \\ \partial_x a &= v, \\ \partial_x b &= w. \end{aligned} \tag{14}$$

The multisymplectic conservation law (6) for the NLS is then given by

$$\partial_t[\boldsymbol{d}a \wedge \boldsymbol{d}b] + \partial_x[\boldsymbol{d}a \wedge \boldsymbol{d}v + \boldsymbol{d}b \wedge \boldsymbol{d}w] = 0. \tag{15}$$

2.1. Local Conservation Laws

One consequence of multisymplecticity is that when the Hamiltonian $S(\boldsymbol{z})$ is independent of x and t, each independent variable gives rise to a conservation law [6]. Conservation of energy and momentum are associated with translation invariance in time and space, respectively. It is easy to show that multiplying (1) with $\boldsymbol{z}_t^T$ from the left provides the energy conservation law (ECL)

$$\partial_t E(\boldsymbol{z}) + \partial_x F(\boldsymbol{z}) = 0, \tag{16}$$

while multiplying (1) with $\boldsymbol{z}_x^T$ from the left yields the momentum conservation law (MCL)

$$\partial_t I(\boldsymbol{z}) + \partial_x G(\boldsymbol{z}) = 0, \tag{17}$$

where

$$\begin{aligned} E(\boldsymbol{z}) &= S(\boldsymbol{z}) - \frac{1}{2}\kappa(\boldsymbol{z}_x, \boldsymbol{z}), \quad F(\boldsymbol{z}) = \frac{1}{2}\kappa(\boldsymbol{z}_t, \boldsymbol{z}), \\ G(\boldsymbol{z}) &= S(\boldsymbol{z}) - \frac{1}{2}\omega(\boldsymbol{z}_t, \boldsymbol{z}), \quad I(\boldsymbol{z}) = \frac{1}{2}\omega(\boldsymbol{z}_x, \boldsymbol{z}), \end{aligned} \tag{18}$$

and κ and ω are defined in (2). Note that $S(\boldsymbol{z})$ itself is not preserved. Implementing relations (16) and (17) for the NLS, one obtains the following energy conservation law (ECL)

$$\partial_t \left[\frac{1}{2}((a^2 + b^2)^2 - v^2 - w^2)\right] + \partial_x(va_t + wb_t) = 0 \tag{19}$$

and momentum conservation law (MCL)

$$\partial_t \left[\frac{1}{2}(aw - vb)\right] + \partial_x \left[\frac{1}{2}((a^2 + b^2)^2 + v^2 + w^2 - (ab_t - a_t b)\right] = 0, \tag{20}$$

respectively. Another conservation law, which we call the norm conservation law for the reason given below, is given by

$$\partial_t \left[\frac{1}{2}(a^2 + b^2)\right] + \partial_x (bv - aw) = 0. \tag{21}$$

These three equations, when integrated with respect to x, yield the classic global conservation of energy (Hamiltonian), momentum, and norm.

3. A MULTISYMPLECTIC SCHEME FOR THE NLS

In a similar spirit to the preservation of the symplectic 2-form by symplectic integrators, multisymplectic integrators are designed to preserve a discrete multisymplectic conservation law. As the multisymplectic structure of PDEs and the use of multisymplectic integrators have only very recently been explored, we provide the following definition from [7]:

Let the discretization of the multisymplectic PDE (1) and the conservation law of multisymplecticity be written schematically as

$$\boldsymbol{M}\partial_t^{i,j}\boldsymbol{z}_i^j + \boldsymbol{K}\partial_x^{i,j}\boldsymbol{z}_i^j = \left(\boldsymbol{\nabla}_{\boldsymbol{z}} S\left(\boldsymbol{z}_i^j\right)\right)_i^j, \tag{22}$$

and

$$\partial_t^{i,j}\omega_i^j + \partial_x^{i,j}\kappa_i^j = 0, \tag{23}$$

respectively, where $\boldsymbol{z}_i^j = \boldsymbol{z}(x_i, t_j)$, $\partial_t^{i,j}$, and $\partial_x^{i,j}$ are discretizations of the corresponding derivatives ∂_t and ∂_x,

$$\omega_i^j = \left\langle \boldsymbol{M}U_i^j, V_i^j \right\rangle \quad \text{and} \quad \kappa_i^j = \left\langle \boldsymbol{K}U_i^j, V_i^j \right\rangle, \tag{24}$$

and

$$\left\{U_i^j\right\}_{(i,j)\in \mathbb{Z}\times\mathbb{Z}}, \left\{V_i^j\right\}_{(i,j)\in \mathbb{Z}\times\mathbb{Z}}$$

are two solutions of the *discrete variational equations*

$$\boldsymbol{M}\partial_t^{i,j}\boldsymbol{dz}_i^j + \boldsymbol{K}\partial_x^{i,j}\boldsymbol{dz}_i^j = \boldsymbol{D}_{\boldsymbol{zz}}^{i,j} S\left(\boldsymbol{z}_i^j\right)\boldsymbol{dz}_i^j.$$

DEFINITION 3.1. The numerical scheme (22) is called a multisymplectic integrator if (23) is a discrete conservation law for (22).

3.1. The Multisymplectic Concatenated Midpoint Rule

Multisymplectic PDEs have a symplectic structure associated with each of the temporal and spatial variables. Thus, a natural starting point for developing multisymplectic schemes is to examine schemes which are known to be symplectic in the traditional sense. One possibility is to concatenate a pair of implicit midpoint discretizations (the simplest symplectic scheme in the Gauss–Legendre family), one in the x-direction and one in the t-direction [7, 20].

Concatenating the two implicit midpoint discretizations (in either order), one obtains the following centered cell discretization of (1)

$$\boldsymbol{M}\left(\frac{\boldsymbol{z}_{i+\frac{1}{2}}^{j+1}-\boldsymbol{z}_{i+\frac{1}{2}}^{j}}{\Delta t}\right)+\boldsymbol{K}\left(\frac{\boldsymbol{z}_{i+1}^{j+\frac{1}{2}}-\boldsymbol{z}_{i}^{j+\frac{1}{2}}}{\Delta_x}\right)=\boldsymbol{\nabla}_{\boldsymbol{z}}S\left(\boldsymbol{z}_{i+\frac{1}{2}}^{j+\frac{1}{2}}\right), \tag{25}$$

where

$$\boldsymbol{z}_{i+\frac{1}{2}}^{j}=\frac{1}{2}\left(\boldsymbol{z}_{i}^{j}+\boldsymbol{z}_{i+1}^{j}\right),\quad \boldsymbol{z}_{i}^{j+\frac{1}{2}}=\frac{1}{2}\left(\boldsymbol{z}_{i}^{j}+\boldsymbol{z}_{i}^{j+1}\right)$$

and

$$\boldsymbol{z}_{i+\frac{1}{2}}^{j+\frac{1}{2}}=\frac{1}{4}\left(\boldsymbol{z}_{i}^{j}+\boldsymbol{z}_{i+1}^{j}+\boldsymbol{z}_{i}^{j+1}+\boldsymbol{z}_{i+1}^{j+1}\right).$$

The centered cell discretization is multisymplectic for any PDE which possesses the multisymplectic formulation (1), i.e., in each cell the discretization satisfies

$$\left(\frac{\omega_{i+\frac{1}{2}}^{j+1}-\omega_{i+\frac{1}{2}}^{j}}{\Delta t}\right)+\left(\frac{\kappa_{i+1}^{j+\frac{1}{2}}-\kappa_{i}^{j+\frac{1}{2}}}{\Delta x}\right)=0 \tag{26}$$

exactly, where ω_i^j and κ_i^j are given by (24) [7].

Applying the centered cell discretization to (14), we obtain the following multisymplectic scheme for NLS:

$$\begin{aligned}
&\frac{b_{i+1/2}^{j+1}-b_{i+1/2}^{j}}{\Delta t}-\frac{v_{i+1}^{j+1/2}-v_{i}^{j+1/2}}{\Delta x}=2\left(\left(a_{i+1/2}^{j+1/2}\right)^2+\left(b_{i+1/2}^{j+1/2}\right)^2\right)a_{i+1/2}^{j+1/2},\\
&\frac{a_{i+1/2}^{j+1}-a_{i+1/2}^{j}}{\Delta t}-\frac{w_{i+1}^{j+1/2}-w_{i}^{j+1/2}}{\Delta x}=2\left(\left(a_{i+1/2}^{j+1/2}\right)^2+\left(b_{i+1/2}^{j+1/2}\right)^2\right)b_{i+1/2}^{j+1/2},\\
&\frac{a_{i+1}^{j+1/2}-a_{i}^{j+1/2}}{\Delta x}=v_{i+1/2}^{j+1/2},\quad \frac{b_{i+1}^{j+1/2}-b_{i}^{j+1/2}}{\Delta x}=w_{i+1/2}^{j+1/2},
\end{aligned} \tag{27}$$

where the following notation has been used (as above in (25))

$$f_{i+1/2}^{j}=\frac{1}{2}\left(f_{i+1}^{j}+f_{i}^{j}\right),\quad f_{i}^{j+1/2}=\frac{1}{2}\left(f_{i}^{j+1}+f_{i}^{j}\right),$$

$$f_{i+1/2}^{j+1/2}=\frac{1}{4}\left(f_{i+1}^{j+1}+f_{i}^{j+1}+f_{i+1}^{j}+f_{i}^{j}\right).$$

For NLS, the corresponding discretization of the multisymplectic conservation law (15) is

$$\frac{da_{i+1/2}^{j+1} \wedge db_{i+1/2}^{j+1} - da_{i+1/2}^{j} \wedge db_{i+1/2}^{j}}{\Delta t} + \frac{da_{i+1}^{j+1/2} \wedge dv_{i+1}^{j+1/2} + db_{i+1}^{j+1/2} \wedge dw_{i+1}^{j+1/2}}{\Delta x} - \frac{da_{i}^{j+1/2} \wedge dv_{i}^{j+1/2} - db_{i}^{j+1/2} \wedge dw_{i}^{j+1/2}}{\Delta x} = 0. \tag{28}$$

Scheme (27), which we denote by MS in the numerical experiments, is second order in space and time. Higher order multisymplectic schemes can be obtained by concatenating higher order members in the Gauss–Legendre family [20]. For completeness, the proof that a concatenated pair of s and r stage (G–L) methods yields a multisymplectic integrator for the NLS equation is provided in the Appendix (Proposition 1). An interesting property of the Gauss–Legendre multisymplectic integrators, when periodic boundary conditions are imposed, is the following

PROPOSITION 3.1. *Let* (14) *be discretized in space and in time by a pair of Gauss–Legendre collocation methods with s and r stages, respectively. The resulting discretization is a multisymplectic integrator for the NLS equation. Further, when periodic boundary conditions are imposed the discretization* (*in particular MS*) *yields a finite dimensional Hamiltonian truncation of the NLS equation in space with the underlying symplectic structure* $\mathbf{d}a \wedge B\mathbf{d}b$ *and a symplectic discretization of this finite-dimensional system in time.* (*See the proof in the Appendix as multisymplectic schemes are not automatically symplectic in the traditional sense.*)

3.2. Discrete Conservation Laws

Applying the centered cell discretization to (16), the corresponding discrete energy conservation law is

$$\frac{E_{i+1/2}^{j+1} - E_{i+1/2}^{j}}{\Delta t} + \frac{F_{i+1}^{j+1/2} - F_{i}^{j+1/2}}{\Delta x} = 0, \tag{29}$$

where

$$\begin{aligned} E_{i+1/2}^{j} &= \frac{1}{2}\left[\left(\left(a_{i+1/2}^{j}\right)^2 + \left(b_{i+1/2}^{j}\right)^2 \right)^2 - \left(\left(v_{i+1/2}^{j}\right)^2 + \left(w_{i+1/2}^{j}\right)^2 \right) \right] \\ F_{i}^{j+1/2} &= v_{i}^{j+1/2}\left(\frac{a_{i}^{j+1} - a_{i}^{j}}{\Delta t} \right) + w_{i}^{j+1/2}\left(\frac{b_{i}^{j+1} - b_{i}^{j}}{\Delta t} \right). \end{aligned} \tag{30}$$

The discrete momentum conservation law takes the form

$$\frac{I_{i+1/2}^{j+1} - I_{i+1/2}^{j}}{\Delta t} + \frac{G_{i+1}^{j+1/2} - G_{i}^{j+1/2}}{\Delta x} = 0, \tag{31}$$

where

$$I_{i+1/2}^{j} = \frac{1}{2}\left(a_{i+1/2}^{j} w_{i+1/2}^{j} - b_{i+1/2}^{j} v_{i+1/2}^{j}\right) \tag{32}$$

$$G_i^{j+1/2} = \frac{1}{2}\Bigg[\left(\left(a_i^{j+1/2}\right)^2 + \left(b_i^{j+1/2}\right)^2\right)^2 + \left(v_i^{j+1/2}\right)^2 + \left(w_i^{j+1/2}\right)^2 - \left(a_i^{j+1/2}\left(\frac{b_i^{j+1} - b_i^j}{\Delta t}\right) - b_i^{j+1/2}\left(\frac{a_i^{j+1} - a_i^j}{\Delta t}\right)\right)\Bigg]. \tag{33}$$

A discrete version of Eq. (21) is given by

$$\frac{N_{i+1/2}^{j+1} - N_{i+1/2}^j}{\Delta t} + \frac{M_{i+1}^{j+1/2} - M_i^{j+1/2}}{\Delta x} = 0, \tag{34}$$

where

$$N_{i+1/2}^j = \frac{1}{2}\left(\left(a_{i+1/2}^j\right)^2 + \left(b_{i+1/2}^j\right)^2\right)$$
$$M_i^{j+1/2} = b_i^{j+1/2}\, v_i^{j+1/2} - a_i^{j+1/2} w_i^{j+1/2}. \tag{35}$$

Reich has shown that multisymplectic Gauss–Legendre schemes preserve both the discrete energy and momentum conservation laws exactly for linear Hamiltonian PDEs (analogous to symplectic Gauss-Legendre schemes preserving the Hamiltonian exactly for linear Hamiltonian ODEs). In the present situation, the local conservation of energy and momentum will not be exact for the NLS using (27) since $S(\boldsymbol{z})$ is not quadratic. However the numerical experiments show that the local conservation laws (19) and (20) are preserved very well over long times.

Integrating the densities $E(\boldsymbol{z})$, $I(\boldsymbol{z})$, and $N(\boldsymbol{z})$ over the spatial domain (with periodic boundary conditions) leads to the global conserved quantities

$$\frac{d}{dt}\mathcal{E}(\boldsymbol{z}) = 0, \quad \frac{d}{dt}\mathcal{I}(\boldsymbol{z}) = 0, \quad \text{and} \quad \frac{d}{dt}\mathcal{N}(\boldsymbol{z}) = 0, \tag{36}$$

where $\mathcal{E}(\boldsymbol{z}) = \int_0^L E(\boldsymbol{z})\, dx$, $\mathcal{I}(\boldsymbol{z}) = \int_0^L I(\boldsymbol{z})\, dx$, and $\mathcal{N}(\boldsymbol{z}) = \int_0^L N(\boldsymbol{z})\, dx$. In the numerical experiments we monitor both the local and global conservation of energy, momentum, and the norm and find that the global momentum and norm are preserved within roundoff. This substantiates that global conservation properties are weaker conditions, i.e., that global conservation of e.g., energy or momentum (36) is a necessary but not sufficient condition for local conservation of energy or momentum (16) and (17). For a further discussion of global versus local conservation properties, see [20].

4. SYMPLECTIC INTEGRATORS FOR THE ABLOWITZ–LADIK DISCRETE NLS SYSTEM

Apart from multisymplectic discretizations, we consider spatial semi-discretizations of NLS that are Hamiltonian with respect to a symplectic structure that is a discrete version of (11) and derive symplectic time integrators for them. The Ablowitz–Ladik (AL) discrete NLS is an obvious choice as it is a completely integrable Hamiltonian system for all N (the discretization parameter) when the conjugacy condition $p_n = \pm q_n^*$ is imposed [1].

4.1. The Ablowitz–Ladik System

The Ablowitz–Ladik discrete NLS system

$$\begin{aligned} i\frac{d}{dt}q_n + \frac{q_{n-1}+q_{n+1}-2q_n}{h^2} + p_n q_n(q_{n-1}+q_{n+1}) = 0 \\ -i\frac{d}{dt}p_n + \frac{p_{n-1}+p_{n+1}-2p_n}{h^2} + p_n q_n(p_{n-1}+p_{n+1}) = 0, \end{aligned} \tag{37}$$

has a noncanonical Hamiltonian form

$$\dot{\boldsymbol{z}} = \boldsymbol{P}(\boldsymbol{z})\nabla H(\boldsymbol{z}), \tag{38}$$

where $\boldsymbol{z} = (\boldsymbol{p}, \boldsymbol{q}) = (p_1, \ldots, p_N, q_1, \ldots, q_N)$ and $\boldsymbol{p} = \boldsymbol{u}^*, \boldsymbol{q} = \boldsymbol{u}$ are the conjugate variables. The Hamiltonian is given by

$$H = \frac{i}{h^3}\sum_{n=1}^{N}[h^2 p_n(q_{n-1}+q_{n+1}) - 2\ln(1+h^2 q_n p_n)], \tag{39}$$

where the Poisson bracket tensor $\boldsymbol{P}(\boldsymbol{z})$ is a $2N \times 2N$ skew-symmetric matrix

$$\boldsymbol{P}(\boldsymbol{z}) = \begin{pmatrix} 0 & -\boldsymbol{R} \\ \boldsymbol{R} & 0 \end{pmatrix}, \quad \boldsymbol{R} = diag[r_1, \ldots, r_N], \quad r_n = \frac{1+h^2 q_n p_n}{h}, \tag{40}$$

so that the fundamental Poisson brackets are given in coordinates (**p**, **q**) by

$$\{p_m, q_n\} = -r_n \delta_{m,n}, \quad \{p_m, p_n\} = \{q_m, q_n\} = 0. \tag{41}$$

The phase space of any Hamiltonian system with a nondegenerate bracket carries a natural symplectic structure. For the AL system (37), the symplectic 2-form is given by

$$\omega(\boldsymbol{p}, \boldsymbol{q}) = \sum_{n=1}^{N} \frac{h}{1+h^2 q_n p_n} dp_n \wedge dq_n. \tag{42}$$

In the continuum limit $h \to 0$ with $p_n = q_n^*$ the Hamiltonian H and the nonstandard Poisson bracket {,} for the AL system approach the Hamiltonian and the standard Poisson bracket, respectively, for the NLS PDE, and the form (42) reduces to the continuous form (11). The AL system inherits all the properties of the original PDE system, and it is possible to derive the N-soliton solution for rapidly decreasing whole-line boundary conditions, as well as quasi-periodic Riemann theta function solutions for periodic boundary conditions [1, 19].

As mentioned above, the AL system carries on its phase space a noncanonical symplectic structure, for which standard symplectic integrators are not immediately applicable. For example, symplectic implicit Runge–Kutta schemes for AL (38) do not exist. We explore several methods for obtaining symplectic schemes for the discrete AL system: (1) we introduce a time dependent coordinate transformation which yields a noncanonical Hamiltonian for which splitting methods can be applied (2) using an additional transformation we reduce the symplectic structure to canonical form and apply standard symplectic schemes and (3) via the generating function method, we develop integrators that preserve the original noncanonical structure (38).

4.2. A Separable Form of the Ablowitz–Ladik System

Under the time-dependent unitary transformation $u_n \mapsto (a_n + ib_n)e^{-2it/h^2}$, the AL system is transformed into another noncanonical Hamiltonian system in *real* coordinates $(\mathbf{a}, \mathbf{b})$ [24]. Letting $w_n(t) = u_n(t)e^{2it/h^2}$, then the new equations of motion are

$$\dot{w}_n = i(w_{n-1} + w_{n+1})\left(\frac{1}{h^2} + |w_n|^2\right). \tag{43}$$

We remark that the equations of motion in this form do not have a well-defined limit as $h \to 0$ since the phase of the right-hand side is then undefined. Scaling of time is necessary to regularize the limit, which is equivalent to a transformation to a system of the original AL form.

Separating $w_n = a_n + ib_n$ into real and imaginary parts, we obtain the following equations of motion in the new real coordinates

$$\dot{a}_n = -c_n(b_{n+1} + b_{n-1}), \quad \dot{b}_n = c_n(a_{n+1} + a_{n-1}), \quad c_n = 1 + h^2\left(a_n^2 + b_n^2\right). \tag{44}$$

These can be cast as a noncanonical Hamiltonian system

$$\dot{Z} = \mathbf{K}(Z)\nabla H(Z), \tag{45}$$

where $Z = \left[\mathbf{a}^T, \mathbf{b}^T\right]^T$, $\mathbf{a} = [a_1, \ldots, a_N]^T$, $\mathbf{b} = [b_1, \ldots, b_N]^T$,

$$\mathbf{K}(Z) = \begin{pmatrix} 0 & -\mathbf{S} \\ \mathbf{S} & 0 \end{pmatrix}$$

with $\mathbf{S} = diag[s_1, \ldots, s_N]$, and $s_n = 1 + h^2(a_n^2 + b_n^2)$ and

$$H = \frac{1}{h^2}\sum_{n=1}^{N}[a_n a_{n+1} + b_n b_{n+1}]. \tag{46}$$

Denoting the right-hand side of (45) by the vector field $V(Z)$, we write the system in the form

$$\dot{Z} = V(Z). \tag{47}$$

A symplectic method for the integration of (47) can be obtained based on the following splitting of V: the vector field V separates into the sum of the A-field

$$\dot{a}_n = -\left(1 + h^2\left(a_n^2 + b_n^2\right)\right)(b_{n+1} + b_{n-1}), \quad \dot{b}_n = 0, \tag{48}$$

and the B-field

$$\dot{a}_n = 0, \quad \dot{b}_n = \left(1 + h^2\left(a_n^2 + b_n^2\right)\right)(a_{n+1} + a_{n-1}). \tag{49}$$

Both systems are Hamiltonian with respect to the same Poisson bracket as (45) and the corresponding Hamiltonians are given by

$$H_A(Z) = \frac{1}{h^2}\sum_{n=1}^{N} a_n a_{n+1}, \quad H_B(Z) = \frac{1}{h^2}\sum_{n=1}^{N} b_n b_{n+1}.$$

Both systems can be trivially integrated. We consider the A-system (48) first and let

$$\bar{B}_n = b_{n-1} + b_{n+1}, \quad B_n^2 = \left(\frac{1}{h^2} + b_n^2\right), \quad A_n = a_n.$$

Then

$$\frac{dA_n}{dt} = -\bar{B}_n\left(B_n^2 + A_n^2\right), \quad \bar{B}_n = const, \ \bar{B}_n = const,$$

which is easily integrated in the form

$$A_n(t) = B_n \frac{\frac{A_n(0)}{B_n} - \tan(B_n \bar{B}_n t)}{1 + \frac{A_n(0)}{B_n}\tan(B_n \bar{B}_n t)}.$$

The B-system (49) is similarly integrated as (with the obvious changes in notation)

$$B_n(t) = A_n \frac{\frac{B_n(0)}{A_n} + \tan(A_n \bar{A}_n t)}{1 - \frac{B_n(0)}{A_n}\tan(A_n \bar{A}_n t)}.$$

We denote the corresponding *symplectic* flow by $\exp At$ and $\exp Bt$. To approximate the flow corresponding to V we can use the Baker–Campbell–Hausdorff formula to expand $\exp(tA + tB)$ in terms of compositions of $\exp tA$ and $\exp tB$, and match the terms up to the given order in t. Additional constraints have to be placed on the expansion coefficients to ensure that the compound flow is symplectic as well. This is done systematically in [17]; we use a well-known second-order symplectic *leapfrog method* that defines a symplectic approximation $\bar{Z}(t)$ to $\exp tV$ as

$$\bar{Z}(t) = \left(\exp \frac{1}{2}tA\right)(\exp tB)\left(\exp \frac{1}{2}tA\right). \tag{50}$$

We denote this integrator by LF.

4.3. The Ablowitz–Ladik System in Canonical Form

In general, any nondegenerate symplectic form can be reduced to the canonical one using a suitable local coordinate transformation. These transformations are not unique since any Darboux transform followed by a symplectic map reduces the system to canonical form. In particular, we consider such transformations for the AL system and upon reduction apply standard symplectic integrators.

We begin with the transformed noncanonical Hamiltonian system (45). Next, standardization of the symplectic structure is accomplished using the Darboux transformation $(\boldsymbol{a}, \boldsymbol{b}) \mapsto (\boldsymbol{c}, \boldsymbol{d})$ given by

$$a_n = \frac{1}{h}\sqrt{1 + h^2 d_n^2}\ \tan\left(h\sqrt{1 + h^2 d_n^2}\, c_n\right).$$
$$b_n = d_n.$$

The AL system can then be rewritten in the canonical form (denoted by the c-AL system)

$$\dot{Y} = \boldsymbol{J}\nabla H(Y), \tag{51}$$

where $Y = [\boldsymbol{c}^T, \boldsymbol{d}^T]^T$, $\boldsymbol{c} = [c_1, \ldots, c_N]^T$, $\boldsymbol{d} = [d_1, \ldots, d_N]^T$,

$$\boldsymbol{J} = \begin{pmatrix} 0 & -\boldsymbol{I} \\ \boldsymbol{I} & 0 \end{pmatrix},$$

with $\boldsymbol{I}$ being the identity matrix and

$$H(\boldsymbol{c}, \boldsymbol{d}) = \frac{1}{h^2} \sum_{n=1}^{N} \left[\frac{1}{h} \sqrt{1 + h^2 d_n^2} \tan\left(h \sqrt{1 + h^2 d_n^2} c_n \right) \right.$$
$$\left. \times \frac{1}{h} \sqrt{1 + h^2 d_{n+1}^2} \tan\left(h \sqrt{1 + h^2 d_{n+1}^2} c_{n+1} \right) + d_n d_{n+1}. \right. \tag{52}$$

The c-AL system can then be discretized in time using standard symplectic schemes such as the second-order implicit midpoint rule (see Section 4.5), and we denote this integrator as CS2.

4.4. Symplectic Schemes for the Noncanonical AL System

An alternate approach to standardization of the symplectic structure is to construct integrators that directly preserve the noncanonical form (42). Since the form (42) is not of potential type, Hamilton–Jacobi theory does not apply. Thus, the most appropriate approach to deriving symplectic integrators for the AL system is based on generating functions [11, 22]. In this section, the method is generalized to generate symplectic integrators of arbitrary order for general noncanonical systems carrying a symplectic structure of the AL type.

We consider symplectic structures given by 2-forms of the type

$$\omega(\mathbf{p}, \mathbf{q}) = \sum_{n=1}^{N} \omega_n(p_n, q_n) dp_n \wedge dq_n,$$

where $\omega_n(p_n, q_n)$ is a function of (p_n, q_n) only. This is perhaps the simplest form of a noncanonical symplectic structure; the standard form is recovered from this expression by setting $\omega_n \equiv 1$. For the AL system, $\omega_n = -r_n^{-1}$. The Poisson bracket dual to ω has the fundamental brackets.

$$\{p_m, q_n\} = -\delta_{m,n,} r_n = -\delta_{m,n} \omega_n^{-1}, \quad \{p_m, p_n\} = \{q_m, q_n\} = 0.$$

and the equations of motion generated by a Hamiltonian function $H(\mathbf{p}, \mathbf{q})$ relative to this bracket have the form

$$\dot{p}_n = -r_n \frac{\partial H}{\partial q_n}, \ \dot{q}_n = r_n \frac{\partial H}{\partial p_n}. \tag{53}$$

A transformation $(\mathbf{p}, \mathbf{q}) \to (\mathbf{P}, \mathbf{Q})$ is called symplectic with respect to ω if

$$\omega(\boldsymbol{p}, \boldsymbol{q}) = \omega(\boldsymbol{P}, \boldsymbol{Q}). \tag{54}$$

Since ω is closed, it is exact, at least locally, and there exists a local primitive 1-form θ, such that $\omega = d\theta$. The primitive is not unique since for any smooth function F the form

$\theta' = \theta + dF$ is also a (local) primitive for ω. One such θ can be obtained by integrating ω with respect to $\mathbf{p}$ along any path in a simply connected neighborhood of $(\mathbf{p}, \mathbf{q})$ as follows

$$\theta(\mathbf{p}, \mathbf{q}) = \boldsymbol{f}d\boldsymbol{q} = \sum_{n=1}^{N} f_n(p_n, q_n)\, dq_n, \quad f_n(P_n, Q_n) = \int_{p_n}^{P_n} \omega_n(\xi, Q_n)\, d\xi.$$

Likewise, integrating with respect to $\mathbf{q}$ obtains another primitive

$$\theta'(\mathbf{p}, \mathbf{q}) = -\boldsymbol{g}d\boldsymbol{p} = -\sum_{n=1}^{N} g_n(p_n, q_n)\, dp_n, \quad g_n(P_n, Q_n) = \int_{q_n}^{Q_n} \omega_n(P_n, \xi)\, d\xi.$$

Given *any* two primitives θ and θ', we can write (54) as

$$d\theta(\mathbf{p}, \mathbf{q}) - d\theta'(\mathbf{P}, \mathbf{Q}) = 0,$$

which means that $\theta(\mathbf{p}, \mathbf{q}) - \theta'(\mathbf{P}, \mathbf{Q})$ is also closed and thus locally exact. Therefore,

$$\theta(\mathbf{p}, \mathbf{q}) - \theta'(\mathbf{P}, \mathbf{Q}) = dG \tag{55}$$

for some smooth function G. In general, (55) characterizes any symplectic map $(\mathbf{p}, \mathbf{q}) \to (\mathbf{P}, \mathbf{Q})$ and the function G is called the *generating function* of the transformation [5]. Equations (55) can be solved for $(\mathbf{P}, \mathbf{Q})$ in the vicinity of the point $(\mathbf{p}, \mathbf{q})$ to obtain an explicit local representation of the transformation. In particular, since the phase flow generated by the equations of motion (53) is a symplectic map for any value of the time parameter, for sufficiently small t we can obtain an explicit representation of the flow in local coordinates $\mathbf{P}, \mathbf{Q}$. We follow Channell and Scovel's approach (see [8]), which uses the transformation equations with a certain generating function $\tilde{G}$ to define the approximate flow so that it is exactly symplectic. The function $\tilde{G}$ is specified by an asymptotic power expansion in t obtained from the equations of motion to ensure the prescribed accuracy of the method. All of the following constructions are local, taking place in a neighborhood of some point $(\mathbf{p}, \mathbf{q})$ where the form ω is assumed nondegenerate and all functions are sufficiently smooth.

Taking the primitives $\theta = \boldsymbol{f}d\boldsymbol{q}$ and $\theta' = -\boldsymbol{g}d\boldsymbol{p}$ obtained above, the transformation equations (55) become

$$\mathbf{f}d\mathbf{q} + \mathbf{g}d\mathbf{P} = dG,$$

or in the component form

$$\frac{\partial G}{\partial q_n} = f_n(p_n, q_n), \quad \frac{\partial G}{\partial P_n} = g_n(P_n, Q_n). \tag{56}$$

Note that G is a generating function of the second kind, i.e., such that

$$\frac{\partial^2 G}{\partial \mathbf{P} \partial \mathbf{q}}$$

is nondegenerate, so we can take $(\mathbf{P}, \mathbf{q})$ to be the local coordinates in the neighborhood of $(\mathbf{p}, \mathbf{q})$. Let $(\mathbf{P}(t), \mathbf{Q}(t))$ be the solution of the system (53) with the initial data $(\mathbf{p}, \mathbf{q})$ and for

sufficiently small t. The right-hand side of the equations of motion

$$\dot{P}_n = -R_n \frac{\partial H}{\partial Q_n}(\mathbf{P},\ \mathbf{Q}), \quad \dot{Q}_n = R_n \frac{\partial H}{\partial P_n}(\mathbf{P},\ \mathbf{Q}), \quad R_n = r_n(P_n,\ Q_n) \tag{57}$$

is smooth in a neighborhood of $(\mathbf{p}, \mathbf{q})$, which justifies asymptotic power expansions in t for $Q_n(t)$ at the point $(\mathbf{p}, \mathbf{q})$. Likewise, smoothness of f_n and g_n and the relations (56) imply the existence of a similar expansion for $G(t)$. Thus, we have asymptotic expressions

$$Q_n(t) = q_n + \underbrace{\sum_{m=1}^{\infty} \frac{t^m}{m!} Q_{m,n}(\mathbf{P}, \mathbf{q})}_{\Delta q_n}, \quad G(t) = \sum_{m=0}^{\infty} \frac{t^m}{m!} G_m(\mathbf{P}, \mathbf{q}) \tag{58}$$

holding in the vicinity of $(\mathbf{p}, \mathbf{q})$. Now we can solve for G in terms of $Q_{n,m}$. To do so, write the second part of the transformation equations as an asymptotic series in t at $(\mathbf{p}, \mathbf{q})$ by expanding g_n in a Taylor series about $\mathbf{q}$ with $\Delta\mathbf{q}$ defined above:

$$\begin{aligned}\sum_{m=0}^{\infty} \frac{t^m}{m!} G_m(\mathbf{P}, \mathbf{q}) &= \sum_{k=0}^{\infty} \frac{1}{k!} \left(\Delta q_n \frac{\partial}{\partial q_n} \right)^k g_n(P_n,\ q_n) \\ &= \sum_{k=0}^{\infty} \frac{1}{k!} \left(\sum_{s=1}^{\infty} \frac{t^s}{s!} Q_{s,n} \frac{\partial}{\partial q_n} \right)^k g_n(P_n,\ q_n).\end{aligned}$$

Expanding the double series obtains an asymptotic series for g_n

$$\begin{aligned}&\sum_{k=0}^{\infty} \frac{1}{k!} \left(\sum_{s=1}^{\infty} \frac{t^s}{s!} Q_{s,n} \frac{\partial}{\partial q_n} \right)^k g_n(P_n,\ q_n) \\ &\quad = \sum_{m=0}^{\infty} t^m \underbrace{\sum_{k=0}^{m} \frac{\partial^k g_n}{\partial q_n^k}(P_n,\ q_n) \sum_{\substack{l_i,\ldots,l_k \geq 0 \\ \sum l_i = m \\ \sum i l_i = k}} \frac{1}{l_1! \ldots l_k!} \left(\frac{Q_{1,n}}{1!} \right)^{l_1} \cdots \left(\frac{Q_{m,n}}{s!} \right)^{l_k}}_{g_{m,n}}\end{aligned}$$

Equating powers of t yields the following relation between the coefficients G_m and $Q_{m,n}$

$$\frac{\partial G_m}{\partial P_n}(\mathbf{P}, \mathbf{q}) = m! \sum_{k=0}^{m} \frac{\partial^k g_n}{\partial q_n^k}(P_n,\ q_n) \sum_{\substack{l_i,\ldots,l_m \geq 0 \\ \sum l_i = k \\ \sum i l_i = m}} \frac{1}{l_1! \ldots l_m!} \left(\frac{Q_{1,n}}{1!} \right)^{l_1} \cdots \left(\frac{Q_{m,n}}{s!} \right)^{l_m} \tag{59}$$

If the $Q_{m,n}$ were known, the G_m could be easily determined by integration. The $Q_{m,n}$ are calculated using the equations of motion as follows. The full-time derivative of Q_n is

$$\dot{Q}_n = \frac{\partial Q_n}{\partial t} + \sum_{j=1}^{N} \frac{\partial Q_n}{\partial P_j} \dot{P}_j,$$

and using (57) it is written

$$\frac{\partial Q_n}{\partial t} = R_n \frac{\partial H}{\partial P_n} + \sum_{j=1}^{N} \frac{\partial Q_n}{\partial P_j} R_j \frac{\partial H}{\partial Q_j}. \tag{60}$$

Next we obtain asymptotic expansions for R_n and the derivatives of H in the same way as was done for g_n above

$$R_n = \sum_{m=0}^{\infty} t^m R_{m,n}(P_n,\ q_n),$$

$$\frac{\partial H}{\partial P_n} = \sum_{m=0}^{\infty} t^m H_{m,P_n}(\mathbf{p},\mathbf{q}), \quad \frac{\partial H}{\partial Q_n} = \sum_{m=0}^{\infty} t^m H_{m,Q_n}(\mathbf{p},\mathbf{q}),$$

with exact expressions for $R_{m,n}$, H_{m,P_n}, and H_{m,Q_n} given in the Appendix. Upon substituting these series into (60), $Q_{m,n}$ can be solved for recursively since a coupling exists among $Q_{m,n}$ such that all the terms appearing on the right-hand side have lower m-indices than that on the left, i.e.,

$$Q_{m+1,n} = m! \left(\sum_{\substack{s+k=m \\ s,k\geq 0}} R_{s,n} H_{k,P_n} + \sum_{\substack{s+k+l=m \\ s\geq 1,\, k,l\geq 0}} \frac{1}{s!} \sum_{j=1}^{N} \frac{\partial Q_{s,n}}{\partial P_j} R_{k,j} H_{l,Q_j} \right). \tag{61}$$

Once $Q_{m,n}$ are obtained and substituted into (59), expressions for G_m are integrated and the generating function G is specified in the form

$$G(\mathbf{P},\mathbf{q}) = \sum_{m=0}^{\infty} \frac{t^m}{m!} G_m(\mathbf{P},\mathbf{q}).$$

It can be calculated to any prescribed accuracy using *any* finite expansion

$$\tilde{G}(t) = \sum_{m=0}^{r} \frac{t^m}{m!} G_m(\mathbf{P},\mathbf{q}), \tag{62}$$

as long as t is sufficiently small. Thus, the truncated function $\tilde{G}(\mathbf{p},\mathbf{q})$ generates the transformation equations

$$f_n(\mathbf{p},\mathbf{q}) = \frac{\partial \tilde{G}}{\partial q_n}(\tilde{\mathbf{P}},\mathbf{q}), \quad g_n(\tilde{\mathbf{P}},\tilde{\mathbf{Q}}) = \frac{\partial \tilde{G}}{\partial \tilde{P}_n}(\tilde{\mathbf{P}},\mathbf{q}), \tag{63}$$

which can be solved for $(\tilde{\mathbf{P}},\tilde{\mathbf{Q}})$ to define a symplectic transformation $(\mathbf{p},\mathbf{q}) \to (\tilde{\mathbf{P}},\tilde{\mathbf{Q}})$ that agrees with the exact flow $(\mathbf{p},\mathbf{q}) \to (\mathbf{P},\mathbf{Q})$ to r-th order. We state this fact as follows:

PROPOSITION 4.2. *Transformation equations* (63) *obtained from a truncated generating function* (62) *can be solved uniquely for sufficiently small t to produce* $(\tilde{\mathbf{P}},\tilde{\mathbf{Q}})$ *such that*

$$(\tilde{\mathbf{P}},\ \tilde{\mathbf{Q}}) = (\mathbf{P},\ \mathbf{Q}) + \mathcal{O}(t^{r+1}), \tag{64}$$

where $(\mathbf{P}, \mathbf{Q})$ *are the solution of the transformation equations with the exact generating function G corresponding to the Hamiltonian flow of the system* (57).

The rather obvious proof of this statement is deferred to the Appendix, while we use this result to derive a second-order symplectic discretization of the AL system.

In the case of the AL system,

$$f_n(p_n,\, q_n) = \frac{1}{hq_n}\ln(1+h^2 p_n q_n), \quad g_n(P_n,\, Q_n) = \frac{1}{hP_n}\ln(1+h^2 P_n Q_n),$$

and using the well-known Taylor series for ln yields an expression of $\frac{\partial G_m}{\partial P_n}$ as obtained from (59)

$$\begin{aligned}
\frac{\partial G_0}{\partial P_n} &= \frac{1}{hP_n}\ln(1+h^2 P_n q_n),\\
\frac{\partial G_m}{\partial P_n} &= \frac{m!}{hP_n}\sum_{k=1}^{m}(-1)^{k-1}(k-1)!\left(\frac{h^2 P_n}{1+h^2 P_n q_n}\right)^k\\
&\quad\times \sum_{\substack{l_i,\ldots,l_m\geq 0\\ \sum l_i = k\\ \sum i l_i = m}} \frac{1}{l_1!\ldots l_m!}\left(\frac{Q_{1,n}}{1!}\right)^{l_1}\cdots\left(\frac{Q_{m,n}}{s!}\right)^{l_m}.
\end{aligned} \tag{65}$$

Next, using the expression for the Hamiltonian and $R_n = \frac{1+h^2 P_n Q_n}{h}$ along with the formulae for their expansion coefficients found in the Appendix, we solve for $Q_{m,n}$ with $m = 1, 2$ and substitute into (64). Except for $m = 0$, these expressions are identified as total derivatives and trivially integrated to yield

$$G_0(\mathbf{P},\, \mathbf{q}) = \sum_{n=1}^{N}\int^{q_n}\frac{1}{hP_n}\ln(1+h^2 P_n\xi)\,d\xi = \sum_{n=1}^{N}\int^{P_n}\frac{1}{hq_n}\ln(1+h^2\xi q_n)\,d\xi,$$

$$G_1(\mathbf{P},\, \mathbf{q}) = H, \quad G_2(\mathbf{P},\, \mathbf{q}) = \sum_j \frac{1}{h}(1+h^2 P_j q_j)\frac{\partial H}{\partial P_j}\frac{\partial H}{\partial q_j}.$$

Substituting the truncated generating function $\tilde{G} = G_0 + tG_1 + \frac{t^2}{2}G_2$ into (63) and solving for $\tilde{P}_n$ and $\tilde{Q}_n$, the following second-order symplectic scheme

$$\begin{aligned}
\tilde{P}_n &= \frac{(1+h^2 q_n p_n)\exp\big(-hq_n\frac{\partial E}{\partial q_n}\big)-1}{h^2 q_n}, \quad E = tG_1 + \frac{t^2}{2}G_2\\
\tilde{Q}_n &= \frac{(1+h^2 q_n \tilde{P}_n)\exp\big(h\tilde{P}_n\frac{\partial E}{\partial \tilde{P}_n}\big)-1}{h^2\tilde{P}_n},
\end{aligned} \tag{66}$$

which we denote (66) by S2. Note that G_0 generates the identity transformation, and its exact expression is not needed.

As the scheme is implicit, to advance one time step from $(\mathbf{p}, \mathbf{q})$ to $(\tilde{\mathbf{P}}, \tilde{\mathbf{Q}})$ the system (66) has to be solved using some type of nonlinear solver. We choose to use a simple fixed-point iteration procedure (FPI), which converges rapidly with a good initial guess given by $(\mathbf{p}, \mathbf{q})$ for all values of t that we used in our numerical experiments.

4.5. Standard Schemes

Standard time integrators are also used in the numerical study below for comparison with the geometric integrators derived in the proceeding sections as well as in the implementation of AL in canonical form. Specifically, we use the explicit second-order Runge–Kutta and the implicit midpoint schemes defined below. Given a dynamical system

$$\dot{\mathbf{z}} = F(\mathbf{z})$$

and initial data $\mathbf{z}$, we compute an approximation $\tilde{\mathbf{Z}}$ at the time t by the explicit second-order Runge–Kutta scheme

$$\tilde{\mathbf{Z}} = \mathbf{z} + tF\left(\mathbf{z} + \frac{t}{2}F(\mathbf{z})\right) \tag{67}$$

and by the implicit midpoint scheme

$$\tilde{\mathbf{Z}} = \mathbf{z} + tF\left(\frac{1}{2}(\mathbf{z} + \tilde{\mathbf{Z}})\right). \tag{68}$$

We denote (67) and (68) by R2 and CS2, respectively. The implicit midpoint rule, CS2, is the lowest order member of the Gauss–Legendre family of implicit Runge–Kutta methods which are symplectic schemes for canonical Hamiltonian systems [13, 21]. Thus, CS2 defines a symplectic transformation when applied to the canonical AL system. As CS2 is implicit, we use the same nonlinear solver (FPI) as with S2 to obtain $\tilde{\boldsymbol{Z}}$ at each time step.

5. NUMERICAL EXPERIMENTS

In this section we examine the performance of the symplectic and multisymplectic methods in solving the NLS equation under periodic boundary conditions $q(x + L,\ t) = q(x,\ t)$ over the time interval $[0,\ T]$ with $T = 500$. For consistency, all the discretizations of the PDE examined are second order in space and time with a fixed time step used throughout the integration. We are interested in simulating multiphase quasi-periodic (in time) solutions. Initial data can be obtained by perturbing the plane wave solution $q_0(x, t) = ae^{2i|a|^2t}$. In the experiments, we use initial data of the form

$$q_n(0) = p_n^*(0) = 0.5(1 + \epsilon\cos(\mu x_n)) \tag{69}$$

for $x_n = -L/2 + (n-1)h,\ h = L/N,\ n = 1, 2, \ldots, N+1$, where $\epsilon = 10^{-2},\ \mu = 2\pi/L$ and L is either (69a) $L = 2\sqrt{2}\pi$ or (69b) $L = 4\sqrt{2}\pi$. The plane wave solution is modulationally unstable and for a fixed amplitude, as the period L is increased, the number of unstable modes increases. Thus, initial data (69a) and (69b) correspond to multiphase solutions, near the plane wave, which are characterized by either one or two excited modes, respectively. For brevity, we will refer to these cases as the one-mode and two-mode case. In almost all the experiments initial data (69a) is used. It is only in the final comparison between the generating function symplectic scheme and the multisymplectic scheme that we consider initial data (69b).

5.1. The Noncanonical AL System: Symplectic Versus Nonsymplectic Integrators

We begin by comparing the performance of the generating function symplectic scheme S2 (66) and the explicit Runge–Kutta scheme R2 (67), applied to the noncanonical AL system (37) for the one-mode case (69a). The numerical schemes are evaluated by monitoring the Hamiltonian H (39), the norm I defined as

$$I(\mathbf{p},\ \mathbf{q}) = \sum_{n=1}^{N} [p_n(q_{n-1} + q_{n+1})], \tag{70}$$

as well as the amplitude of the waveform of the solution.

Figures 1a and 1b show the error in the Hamiltonian obtained using S2 and R2 for (a) $N = 4$ with $t = 10^{-2}$ and for (b) $N = 32$ with $t = 10^{-3}$. The symplectic scheme S2 preserves the Hamiltonian extremely well during long time integrations as the error in the Hamiltonian oscillates in a bounded fashion and does not exhibit a linear drift as it does with R2. However, the linear error growth in H which occurs using the nonsymplectic method becomes less significant as the time step t decreases and the dimension of the system N increases (compare Figs. 1a and 1b).

This behavior is summarized in Table I which provides the maximum error in H of the AL system as a function of N and t using schemes S2 and R2, i.e., for mesh sizes $N = 4,\ 16,\ 32,$

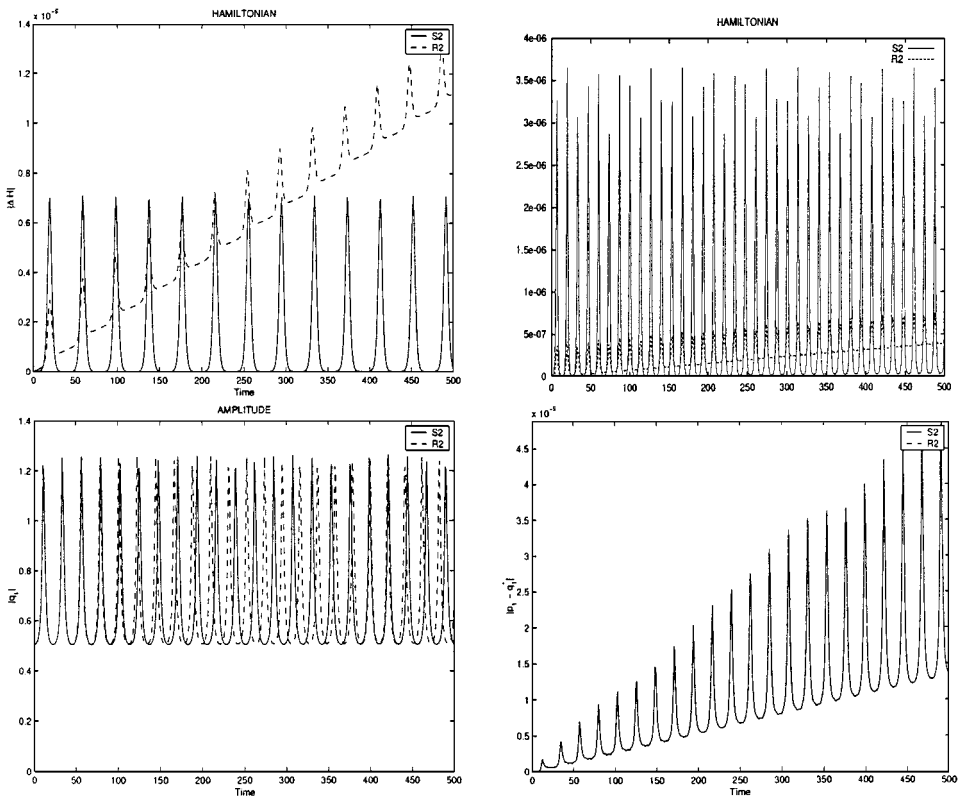

FIG. 1. Comparison of integrators S2 and R2 for the noncanonical AL system: (a) error in the Hamiltonian for $N = 4$ with $t = 10^{-2}$, (b) error in the Hamiltonian for $N = 32$ with $t = 10^{-3}$, (c) Amplitude of q_1 for $N = 16$ with $t = 10^{-2}$, (d) Conjugacy deviation $|\mathbf{p}_1 - \mathbf{q}_1^*|$ for $N = 16$ with $t = 10^{-3}$.

TABLE I
Maximum Absolute Error in the AL Hamiltonian Obtained with S2 and R2 for $T = 500$

N	4	4	16	16	32	32	64	64
t	1.0E-02	1.0E-03	1.0E-02	1.0E-03	1.0E-03	1.0E-04	5.0E-04	1.0E-04
S2	7.1E-06	7.1E-08	2.7E-04	2.7E-06	3.7E-06	5.1E-08	1.0E-06	1.0E-07
R2	1.3E-05	3.5E-08	2.2E-04	5.2E-07	6.0E-07	4.1E-09	1.2E-07	4.1E-09

and 64, each for two time steps. The preservation of the second invariant I is not presented as it is qualitatively similar to H. The experiments with different time steps t indicate that the error in the Hamiltonian is bounded by $\gamma_{S2}t^2$ for the method S2, whereas it behaves like $\alpha_{R_2}t^2 + \beta_{R_2}Tt^3$ for the method R2. The dependence of the constants γ_{S2}, α_{R_2}, and β_{R_2} on the space discretization parameter h is less clear (see Table I).

Figure 1c shows the amplitude of q_1 of the solution obtained with the two integrators R2 and S2 using $N = 16$ and $t = 10^{-2}$. Solutions of the AL system exhibit regular quasi-periodic motion because of the fact that the AL flow occurs in general on an N-torus. For $t = 0.01$, a phase lag develops using R2 which becomes more pronounced as the system evolves. However, using $t = 0.001$ the solutions from the two integrators are virtually indistinguishable on the time scale examined. The amplitudes of the other lattice sites show similar qualitative behavior.

The conjugacy relation $\mathbf{q} = \mathbf{p}^*$ arises in the applications of the NLS of physical interest [9, 25], thus preserving this additional constraint can potentially be as important as preserving the symplectic structure. It is of interest then to consider initial data of this form and to determine which of the schemes minimizes $|\mathbf{p} - \mathbf{q}^*|$, the deviation from conjugacy. Figure 1d shows that the deviation in $|p_1 - q_1^*|$ for N = 16 and $t = 10^{-3}$ is of size 10^{-6} using S2, whereas with R2 it is on the order of roundoff (the deviation in $|p_n - q_n^*|$ is comparable for general n). Note: Although $\mathbf{q}(0) = \mathbf{p}^*(0)$ and the semidiscrete AL flow preserves conjugacy, this condition is not imposed throughout the time evolution as the performance of the integrator degrades. In fact, if the relation is imposed and the implicit scheme is solved for just q_n at each time step, a linear error growth in the Hamiltonian occurs indicating that in this case the scheme is not symplectic [22].

Both schemes exhibit stability issues as can be seen from the $N = 4$ and $N = 16$ cases. Keeping the time step fixed and varying N (equivalently h), as h decreases the performance of both schemes degrades. This suggests that $t/h^2 < M$, for some M, is required for stability. The instability is more pronounced for the explicit scheme R2 than for either of the symplectic schemes. It is surprising then that R2 preserves conjugacy better, indicating that instabilities of R2 lie in the $\mathbf{p} = \mathbf{q}^*$ subspace, whereas for S2 they are transverse to it.

It should be mentioned that R2, being an explicit scheme, is faster than S2 and the difference in computation time becomes more significant as the dimension $2N$ of the semi-discrete system is increased. At the same time, the difference in accuracy of the two schemes manifests on a longer time scale, making $R2$ attractive for intermediate integration times.

5.2. The Symplectic Integrators in Noncanonical and Canonical Form

Next we compare the performance of the leapfrog method LF (50), the symplectic canonical implicit midpoint scheme CS2 (68) and the generating function symplectic scheme S2

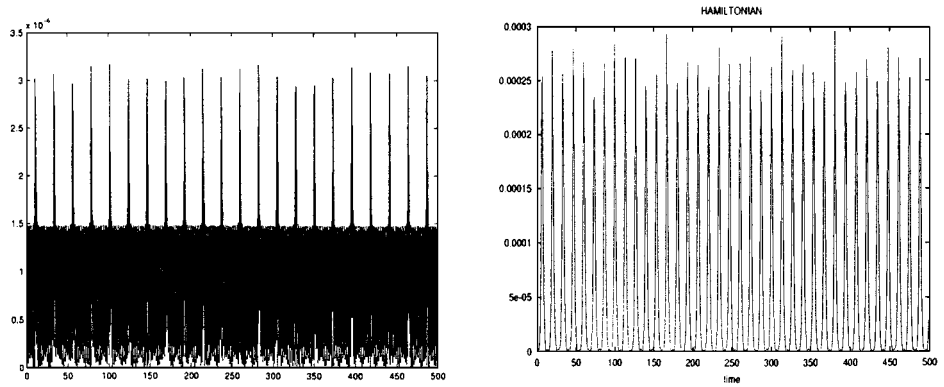

FIG. 2. The error in the Hamiltonian, for $T = 500$, obtained with (a) the LF integrator using $N = 32$, $t = 10^{-4}$ and (b) the canonical AL integrator using $N = 32$, $t = 10^{-3}$.

(66) for the one-mode case (69a). Initialization and comparison of the constants of motion and waveform for the various integration methods is done in the original coordinate system $(\mathbf{p}, \mathbf{q})$, i.e., we unwind all transformations before the AL Hamiltonian (39) is computed and output is generated. For the implicit schemes, the same criterion is used to accept a solution of the iterative procedure at each time step, namely, the L_1-norm of the error has to be less than 10^{-10}.

Both LF and CS2 exhibit the characteristic behavior of symplectic schemes. As an example, Fig. 2 shows the error in the Hamiltonian, which is nicely bounded over long times obtained with (a) LF using $N = 32$, $t = 10^{-4}$ and (b) CS2 using $N = 32$, $t = 10^{-3}$, both for $T = 500$. Table II provides the maximum absolute error in the AL Hamiltonian (39) obtained with the symplectic schemes CS2, S2, and LF for mesh sizes $N = 32$ and 64, each for two time steps. For fixed h ($h = L/N$), halving the time step results in a decrease in the maximum error in H by a factor of 2^{-2}. An example of this is shown in the table for $N = 32$. This supports the conjecture that for the LF and CS2 methods, the error in H is bounded by $\gamma_{LF}t^2$ and $\gamma_{CS2}t^2$, respectively, similar to the results for S2. However, the maximum error in H obtained with LF and CS2 is at least two orders of magnitude larger than with S2. Thus, the error coefficients γ_{LF}, γ_{CS2} are significantly larger than γ_{S2}. In Fig. 2a, small amplitude, high-frequency background oscillations are visible against the dominant large amplitude, low-frequency oscillations (whose frequency corresponds to that of the excited mode in the AL solution). The time-dependent map $u \mapsto w$ is responsible for the high-frequency oscillations as well as the less accurate resolution of the Hamiltonian exhibited by LF and CS2.

TABLE II
Maximum Absolute Error in the AL Hamiltonian Obtained Using the Symplectic Schemes CS2, S2, and LF for $T = 500$

N	32	32	64	64
t	2.0E-03	1.0E-03	5.0E-04	1.0E-04
CS2	1.2E-03	3.0E-04	1.0E-03	4.5E-05
S2	1.5E-05	3.7E-06	1.0E-06	1.0E-07
LF	1.3E-03	3.2E-04	1.6E-03	6.4E-05

In the experiments, CS2 was found to be less efficient than S2 as it requires almost as much CPU time as S2 even though it is less accurate. On the other hand, LF is relatively fast and easy to implement but is also less accurate than S2. In addition, the method is based on a particular feature of (44)—its separable nature, which is not apparent from the original AL formulation, nor general enough. Although there is no loss of conjugacy when using LF and CS2, we emphasize the utility of the generating function method for its ability to handle a wide class of noncanonical Hamiltonian systems. To obtain a robust symplectic integrator which preserves $p_n = q_n^*$ exactly, the conjugacy condition should be imposed first. Then letting $q_n = a_n + ib_n$, the AL system can be written in real form and the generating function method developed in Section 4 applied to the real noncanonical system.

5.3. The Multisymplectic Integrator

Lastly, we consider the multisymplectic scheme MS. As before, we use initial conditions (69a) and examine the performance of the scheme for different mesh sizes and time steps (see Table III). The multisymplectic discretization (27) is implicit and can be solved using iteration schemes. All the local conservation laws are of the general form

$$\partial_t T + \partial_x F = 0, \tag{71}$$

and multiplying the discrete conservation laws (29)–(31) by $\Delta x \Delta t$, they can be written as

$$\left(T_{i+1/2}^{j+1} - T_{i+1/2}^{j}\right)\Delta x + \left(F_{i+1}^{j+1/2} - F_{i}^{j+1/2}\right)\Delta t = 0. \tag{72}$$

In addition to the local energy and momentum conservation laws, we monitor the error in the global invariants $\mathcal{E}(t)$, $\mathcal{I}(t)$, and $\mathcal{N}(t)$. Once the local conservation laws (29)–(31) have been evaluated, we obtain a second-order approximation to the global conserved quantities by implementing (72) and summing in space and time.

Figure 3 provides the results obtained using MS for initial data (69a), with $N = 64$ and $t = 5 \times 10^{-3}$ over the time interval [0, 500]. For clarity, in the surface plots we only show the time slice [450, 500]. The surface of the one mode multiphase solution (Fig. 3a) displays quasiperiodic behavior in time. Figures 3b and 3c show the errors in the local energy and momentum conservation laws as given by (29)–(31). The errors in the local conservation laws are concentrated in the regions of the multiphase solution where there are steep gradients. The corresponding error in the global energy and momentum over the time interval [0, 500] are given in Figs. 3d and 3e. It is worth noting that the global momentum and norm (not shown) are conserved *exactly* (up to the error criterion of 10^{-14} in the iteration procedure in the implicit MS scheme) since they are quadratic invariants! Clearly, this is a very attractive feature of the MS scheme. Further, the error in the global energy oscillates in a bounded fashion as is typical of the behavior of a symplectic integrator (recall Proposition 1, where MS is shown to be symplectic).

The maximum error in the local energy and momentum and global energy and momentum for the multisymplectic scheme are provided in Table III for mesh sizes $N = 32$ and 64, each for three time steps. From the experiments it is readily seen that the error in the local energy conservation law (29) depends only on the time step t and that the the error is second order in t (successively halving the time step decreases the LE error each time by a factor of 2^{-2}). In contrast, the error in the local momentum conservation law (31) depends only on the spatial mesh size N and, as anticipated, the error in LM is second order in h.

TABLE III

The Absolute Maximum Error in the Local Energy and Momentum and the Global Energy and Momentum Obtained Using the Multisymplectic Scheme MS, with $T = 500$

N	32	32	32	64	64	64
t	2.0E-02	1.0E-02	5.E-03	2.0E-02	1.0E-02	5.0E-03
LE	6.0E-05	1.5E-05	4.0E-06	8.0E-05	2.0E-05	5.0E-06
LM	1.7E-02	1.7E-02	1.7E-02	4.8E-03	4.8E-03	4.8E-03
GE	7.3E-05	2.0E-05	5.0E-06	7.6E-05	2.2E-05	5.0E-06
GM	1.2E-13	2.5E-14	2.0E-13	1.3E-13	1.0E-13	4.5E-13

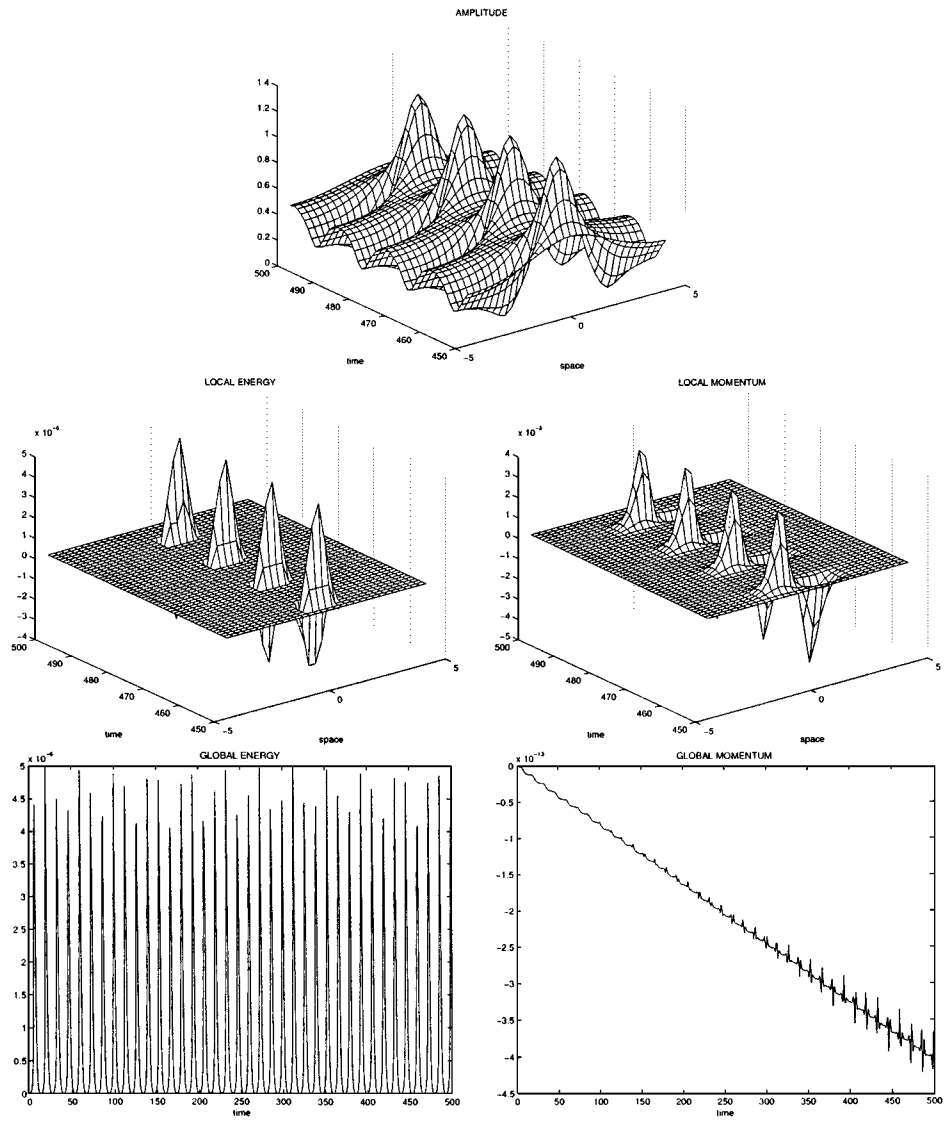

FIG. 3. The multisymplectic scheme MS with $N = 64$ and $t = 5 \times 10^{-3}$, $T = 500$: (a) surface, (b–c) error in the local energy and momentum conservation law, respectively, (d–e) error in the global energy and momentum, respectively.

The approximation to the global energy, GE, obtained using the MS scheme and the Hamiltonian for the AL system both provide a second-order approximation to the NLS Hamiltonian. In comparing the error in the GE in Table III with the errors in the Hamiltonian in Tables I and II we see that the multisymplectic scheme preserves the global energy better than both S2 and CS2. So in addition to having very good resolution of the local conservation laws, the multisymplectic scheme preserves the global energy extremely well (and the global momentum and norm exactly!). Another important feature of the MS method is that it is significantly faster than the symplectic schemes S2 and CS2.

A final issue to consider is the preservation of the qualitative properties of the solution. Since to consider S2 to be the most robust of the symplectic integrators for the AL system, we compare the performance of MS with that of S2. As mentioned before, the surface of the waveform obtained using MS for initial data (69a) with discretization parameters $N = 64$, $t = 5 \times 10^{-3}$ is given in Fig. 3a for the time frame $450 < t < 500$. Implementing S2 with the same discretization parameters and for the same initial data, the surface of the waveform appears identical to Fig. 3a. This is initial data for a stable multiphase solution of NLS and, although "near" the unstable plane wave solution, it is not "too close" (as measured in spectral space; see [3]). It is expected that when simulating other stable solutions of NLS, e.g., solitons (which are actually a limiting case of the multiphase solutions with $L \to \infty$), the MS and S2 schemes will comparably preserve the qualitative features of the waveform. However, when examining more complex solutions there can be a striking difference in the

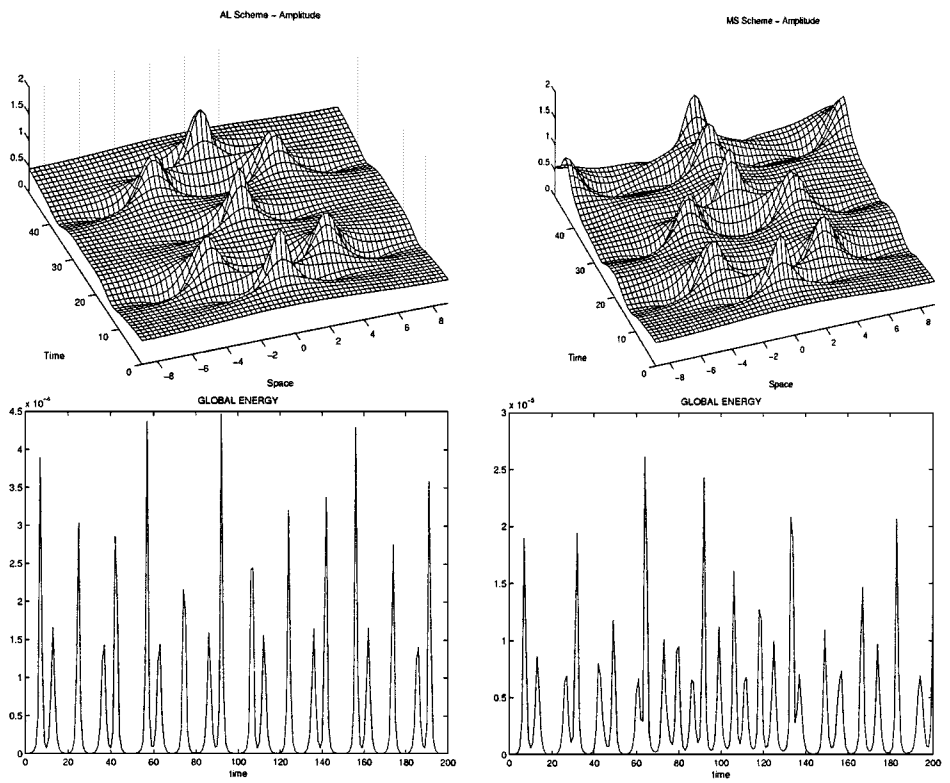

FIG. 4. The two mode multiphase solution with $N = 64$, $t = 5 \times 10^{-3}$ and $T = 500$: (a–b) the surface of the waveform obtained using the S2 and the MS discretization, respectively and (c–d) the error in the global energy obtained using the S2 and the MS discretization, respectively, for initial data (69b).

S2 and MS results. In highly sensitive regimes, where the proximity to unstable solutions and numerically induced chaos is an important computational issue, the integrability of the AL discretization beomes crucial. Figure 4 shows (a-b) the surface of the waveform and (c-d) the error in the global energy obtained using the S2 and the MS discretization, respectively, for initial data (69b) with discretization parameters $N = 64$, $t = 5 \times 10^{-3}$, and $T = 500$. Notice that the AL based S2 scheme accurately captures the quasiperiodic motion. On the other hand, using the MS integrator, the onset of numerically induced temporal chaos is observed. A random switching in time of the location of the spatial excitations in the waveform is clearly visible, even though MS preserves the global energy better than AL (see Figs. 4c and 4d). As a consequence, for sensitive regimes, the significant improvement in the qualitative features of the waveform obtained with the integrable AL-S2 scheme justifies the computational expense. The advantages of the MS scheme are as follows—when considering nonsensitive regimes such as the one-mode multiphase solution, it is faster, there is no loss of conjugacy, it handles a wide range of mesh size and it preserves the local conservation laws and global invariants as well or better than S2.

6. CONCLUSIONS

In this paper we have analyzed and developed various geometric integrators for the NLS system. The numerical experiments indicate that when compared to traditional integrators, represented by a Runge–Kutta method R2, geometric schemes are generally more efficient in preservation of geometric features of the system, such as local and global conserved quantities (actions), quasiperiodic character of the motion and qualitative features of the waveform. At the same time, geometric integrators typically result in highly nonlinear implicit schemes that are slower than the more straightforward explicit R2. In addition, various relative advantages of some geometric integrators become less pronounced as the values of discretization parameters h and t tend to zero, approximating the PDE, while their relative run-time performance degrades further. In this regard, the multisymplectic scheme is an exception since its accuracy improves as the PDE limit is approached and the run-time performance does not suffer substantially.

It is important to emphasize that geometric integrators do reproduce several qualitative features of NLS better than R2. In particular, they preserve the action values much better as the deviations in the integrals from the initial values stay bounded, while R2 produces essentially linear drifts. The implications are that for very long time simulations, important for statistical studies of the NLS system and its perturbations, geometric integrators provide an effective tool. Indeed, averaged quantities obtained with such schemes are much more likely to reflect those of the original system than the statistics obtained with R2 because of uncompensated mean drifts. In this situation, the extra cost associated with geometric schemes is well worth the result.

Among the geometric schemes, performance varied for different parameter values and initial data. The multisymplectic scheme seems to be the best in terms of run-time performance and the quality of preservation of the local and global integrals of motion. At the same time, using initial data for the two mode multiphase solutions of NLS, MS fails to capture the proper PDE waveform despite excellent integral preservation. In contrast, symplectic schemes for the AL system never preserve integrals to the same degree but faithfully reproduce the qualitative features of the wave profile and the quasiperiodic character of the motion.

To obtain symplectic integrators for the integrable semi-discretization of NLS, the AL system, we extended the canonical procedure based on generating functions to a fairly wide class of noncanonical systems carrying a symplectic structure of the AL type and potentially a much wider class of systems. The integrators derived from this generating function technique appear to be very robust and provide a rather general tool for nonlinear Hamiltonian systems. This is in contrast with methods based on vector field splitting which appear less general in this setting.

In summary, geometric integrators provide an "expensive" but valuable tool for studies of long time behavior of nonlinear PDEs, and different schemes are preferred in different parameter regimes and for different initial data. The approach to construction of such integrators via generating functions appears to be fairly general and robust. The newly emerging class of multisymplectic integrators for nonlinear wave equations also proved extremely promising, although limits of applicability of this method are still to be precisely determined, as it includes simple and fast schemes with remarkable conservation properties for local as well as global invariants.

APPENDIX I: PROOF OF PROPOSITION 1

PROPOSITION A.1. *Let* (14) *be discretized in space and in time by a pair of Gauss–Legendre collocation methods with s and r stages*, *respectively. The resulting discretization is a multisymplectic integrator for the NLS equation. Further*, *when periodic boundary conditions are imposed the discretization yields a finite dimensional Hamiltonian truncation of the NLS equation in space with the underlying symplectic structure* $da \wedge Bdb$ *and a symplectic discretization of this finite-dimensional system in time.*

As in [20], we begin by discretizing in space and apply an implicit s-stage Runge–Kutta scheme to the multisymplectic formulation of NLS (14) to obtain the spatial semi-discretization,

$$
\begin{aligned}
A_i &= a_k + \Delta x \sum_{j=1}^{s} \tilde{a}_{ij} V_j, \\
V_i &= v_k + \Delta x \sum_{j=1}^{s} \tilde{a}_{ij} \left(-\partial_t B_j - 2\left(A_j^2 + B_j^2\right) A_j\right), \\
B_i &= b_k + \Delta x \sum_{j=1}^{s} \tilde{a}_{ij} W_j, \\
W_i &= w_k + \Delta x \sum_{j=1}^{s} \tilde{a}_{ij} \left(\partial_t A_j - 2\left(A_j^2 + B_j^2\right) B_j\right), \\
a_{k+1} &= a_k + \Delta x \sum_{j=1}^{s} \tilde{b}_j V_j, \\
v_{k+1} &= v_k + \Delta x \sum_{j=1}^{s} \tilde{b}_j (-\partial_t B_j - 2(A^2 + B^2) A),
\end{aligned}
\tag{A.1}
$$

$$b_{k+1} = b_k + \Delta x \sum_{j=1}^{s} \tilde{b}_j W_j,$$
$$w_{k+1} = w_k + \Delta x \sum_{j=1}^{s} \tilde{b}_j (\partial_t A_j - 2(A^2 + B^2)B),$$

which is defined for all t. The standard notation $u_k(t) \approx u(x_k, t)$ is employed, and for convenience we set $k = 0$ and assume that $x_k = 0$. The corresponding semi-discretization of conservation law (15) is given by

$$[\boldsymbol{d}a_1 \wedge \boldsymbol{d}v_1 - \boldsymbol{d}a_0 \wedge \boldsymbol{d}v_0] + [\boldsymbol{d}b_1 \wedge \boldsymbol{d}w_1 - \boldsymbol{d}b_0 \wedge \boldsymbol{d}w_0] + \sum_{i=1}^{s} \tilde{b}_i \partial_t [\boldsymbol{d}A_i \wedge \boldsymbol{d}B_i] \Delta x = 0. \tag{A.2}$$

Solving the first four equations of (A.1) for $\partial_t A_j$, $\partial_t B_j$, $j = 1, \ldots, s$, we next implement an r-stage Runge–Kutta discretization in time

$$\begin{aligned} A_{i,m} &= a_i^0 + \Delta t \sum_{n=1}^{r} \tilde{\tilde{a}}_{mn} \partial_t A_{i,n}, \quad B_{i,m} = b_i^0 + \Delta t \sum_{n=1}^{r} \tilde{\tilde{a}}_{mn} \partial_t B_{i,n}, \\ a_i^1 &= a_i^0 + \Delta t \sum_{n=1}^{r} \tilde{\tilde{b}}_m \partial_t A_{i,m}, \quad b_i^1 = b_i^0 + \Delta t \sum_{n=1}^{r} \tilde{\tilde{b}}_m \partial_t B_{i,m}, \end{aligned} \tag{A.3}$$

with the corresponding conservation property

$$\left[\boldsymbol{d}a_i^1 \wedge \boldsymbol{d}b_i^1 - \boldsymbol{d}a_i^0 \wedge \boldsymbol{d}b_i^0\right] - \sum_{m=1}^{r} \tilde{\tilde{b}}_m [\partial_t \boldsymbol{d}A_{i,m} \wedge \boldsymbol{d}B_{i,m} + \boldsymbol{d}A_{i,m} \wedge \partial_t \boldsymbol{d}B_{i,m}] \Delta t = 0. \tag{A.4}$$

Combining (A.1) and (A.3), the discretized multisymplectic conservation law is given by

$$\begin{aligned} &\sum_{i=1}^{s} \tilde{b}_i \left[\boldsymbol{d}a_i^1 \wedge \boldsymbol{d}b_i^1 - \boldsymbol{d}a_i^0 \wedge \boldsymbol{d}b_i^0\right] \Delta x + \sum_{m=1}^{r} \tilde{\tilde{b}}_m \left[\boldsymbol{d}a_1^m \wedge \boldsymbol{d}v_1^m - \boldsymbol{d}a_0^m \wedge \boldsymbol{d}v_0^m \right. \\ &\quad \left. + \boldsymbol{d}b_1^m \wedge \boldsymbol{d}w_1^m - \boldsymbol{d}b_0^m \wedge \boldsymbol{d}w_0^m\right] \Delta t = 0, \end{aligned} \tag{A.5}$$

which is a discretization of (15) integrated over the domain $[0, \Delta x] \times [0, \Delta t]$. This establishes that the concatenated G–L integrator is multisymplectic.

To examine a global property such as symplecticity, sum over the k lattice points:

$$\begin{aligned} &\sum_{k=1}^{M} \left(\sum_{i=1}^{s} \bar{b}_i \left[\boldsymbol{d}a_{i,k}^1 \wedge \boldsymbol{d}b_{i,k}^1 - \boldsymbol{d}a_{i,k}^0 \wedge \boldsymbol{d}b_{i,k}^0\right] \Delta x + \sum_{m=1}^{r} \tilde{\tilde{b}}_m \left[\boldsymbol{d}a_{k+1}^m \wedge \boldsymbol{d}v_{k+1}^m - \boldsymbol{d}a_k^m \wedge \boldsymbol{d}v_k^m \right. \right. \\ &\quad \left. \left. + \boldsymbol{d}b_{k+1}^m \wedge \boldsymbol{d}w_{k+1}^m - \boldsymbol{d}b_k^m \wedge \boldsymbol{d}w_k^m\right] \Delta t \right) = 0. \end{aligned} \tag{A.6}$$

Expanding the outer sum and noting that for periodic boundary conditions $a^m_{M+1} = a^m_1$ and $v^m_{M+1} = v^m_1$, we find

$$\sum_{k=1}^{M}\sum_{m=1}^{r}\tilde{\tilde{b}}_m\left[\boldsymbol{d}a^m_{k+1}\wedge\boldsymbol{d}v^m_{k+1}-\boldsymbol{d}a^m_k\wedge\boldsymbol{d}v^m_k\right]\Delta t$$
$$=\sum_{m=1}^{r}\tilde{\tilde{b}}_m\left[\boldsymbol{d}a^m_{M+1}\wedge\boldsymbol{d}v^m_{M+1}-\boldsymbol{d}a^m_1\wedge\boldsymbol{d}v^m_1\right]\Delta t=0. \tag{A.7}$$

Similarly,

$$\sum_{k=1}^{M}\sum_{m=1}^{r}\tilde{\tilde{b}}_m\left[\boldsymbol{d}b^m_{k+1}\wedge\boldsymbol{d}w^m_{k+1}-\boldsymbol{d}b^m_k\wedge\boldsymbol{d}w^m_k\right]\Delta t=0.$$

Therefore,

$$\sum_{k=1}^{M}\sum_{i=1}^{s}\tilde{b}_i\left[\boldsymbol{d}a^1_{i,k}\wedge\boldsymbol{d}b^1_{i,k}\right]=\sum_{k=1}^{M}\sum_{i=1}^{s}\tilde{b}_i\left[\boldsymbol{d}a^0_{i,k}\wedge\boldsymbol{d}b^0_{i,k}\right]. \tag{A.8}$$

This is conservation of symplecticity in time with respect to the state variables $a=\{a_{i,k}\}$ and $b=\{b_{i,k}\}$ and the wedge product $\boldsymbol{d}a\wedge\tilde{B}\boldsymbol{d}b$, where $\tilde{B}$ is a diagonal matrix with entries $\{\bar{b}_i\}$.

APPENDIX 2. FORMULAE FOR THE NONCANONICAL SYMPLECTIC INTEGRATOR

Substituting $\mathbf{Q}=\mathbf{q}+\Delta\mathbf{q}$ allows the derivatives of H and R_n to be expanded in power series in t with all coefficients evaluated at $(\mathbf{P},\mathbf{q})$ the same way it was done for g_n in the text.

$$\frac{\partial H}{\partial P_n}(\mathbf{P},\mathbf{Q})=\sum_{k=0}^{\infty}\frac{1}{k!}\left(\Delta\mathbf{q}\frac{\partial}{\partial\mathbf{q}}\right)^k\frac{\partial H}{\partial P_n}(\mathbf{P},\mathbf{q}),$$

where formally

$$\sum_{k=0}^{\infty}\frac{1}{k!}\left(\Delta\mathbf{q}\frac{\partial}{\partial\mathbf{q}}\right)^k=\exp\left(\Delta\mathbf{q}\frac{\partial}{\partial\mathbf{q}}\right)$$

is the shift operator $\mathbf{q}\to\mathbf{q}+\Delta\mathbf{q}$ that generates its Taylor expansion for any smooth function of $\mathbf{q}$. Here

$$\Delta\mathbf{q}\frac{\partial}{\partial\mathbf{q}}\equiv\sum_{j=1}^{N}\Delta q_j\frac{\partial}{\partial q_j},$$

so that

$$\left(\Delta\mathbf{q}\frac{\partial}{\partial\mathbf{q}}\right)^k\frac{\partial H}{\partial P_n}(\mathbf{p},\mathbf{q})=\sum_{j_1,\ldots,j_k=1}^{N}\frac{\partial^{k+1}H}{\partial P_n\partial q_{j_1}\ldots\partial q_{j_k}}\Delta q_{j_1}\ldots\Delta_{j_k}$$
$$=\sum_{j_1,\ldots,j_k=1}^{N}\frac{\partial^{k+1}H}{\partial P_n\partial q_{j_1}\ldots\partial q_{j_k}}\left(\sum_{s=1}^{\infty}\frac{t^s}{s!}Q_{s,j_1}\right)\cdots\left(\sum_{s=1}^{\infty}\frac{t^s}{s!}Q_{s,j_k}\right).$$

With this notation we obtain

$$\frac{\partial H}{\partial P_n} = \sum_{s=0}^{\infty} t^s \underbrace{\sum_{k=0}^{s} \sum_{j_1,\ldots,j_k=1}^{N} \frac{\partial^{k+1} H}{\partial P_n \partial q_{j_1} \ldots \partial q_{j_k}} \sum_{\substack{l_i,\ldots,l_s \geq 0 \\ \sum l_i = k \\ \sum i l_{i=s}}} \frac{1}{l_1! \ldots l_s!} \left(\frac{Q_{1,j_1}}{1!}\right)^{l_1} \cdots \left(\frac{Q_{s,j_k}}{s!}\right)^{l_s}}_{H_{s,P_n}}. \tag{A.9}$$

Likewise,

$$\frac{\partial H}{\partial Q_n} = \sum_{s=0}^{\infty} t^s \underbrace{\sum_{k=0}^{s} \sum_{j_1,\ldots,j_k=1}^{N} \frac{\partial^{k+1} H}{\partial q_n \partial q_{j_1} \ldots \partial q_{j_k}} \sum_{\substack{l_i,\ldots,l_s \geq 0 \\ \sum l_i = k \\ \sum i l_i = s}} \frac{1}{l_1! \ldots l_s!} \left(\frac{Q_{1,j_1}}{1!}\right)^{l_1} \cdots \left(\frac{Q_{s,j_k}}{s!}\right)^{l_s}}_{H_{s,Q_n}}, \tag{A.10}$$

and

$$R_n(P_n,\ Q_n) = \sum_{m=0}^{\infty} t^m \underbrace{\sum_{k=0}^{m} \frac{\partial^k R_n}{\partial Q_n^k}(P_n,\ q_n) \sum_{\substack{l_i,\ldots,l_k \geq 0 \\ \sum l_i = m \\ \sum i l_i = k}} \frac{1}{l_1! \ldots l_k!} \left(\frac{Q_{1,n}}{1!}\right)^{l_1} \cdots \left(\frac{Q_{m,n}}{s!}\right)^{l_k}}_{R_{m,n}}, \tag{A.11}$$

In the case of the AL system $R_n(P_n, Q_n) = \frac{1}{h}(1 + h^2 P_n Q_n)$ so that

$$R_n(P_n, Q_n) = \underbrace{\frac{1 + h^2 P_n q_n}{h}}_{R_{0,n}} + \sum_{s=1}^{\infty} t^s \underbrace{\frac{1}{s!} h P_n Q_{s,n}}_{R_{s,n}}. \tag{A.12}$$

APPENDIX 3. PROOF OF PROPOSITION 2

PROPOSITION A.2. *Consider the Taylor series expansions for the generating function G of the phase flow of the system* (57) *and its r-th order truncation $\tilde{G}$*

$$G(t) = \sum_{m=0}^{\infty} \frac{t^m}{m!} G_m(\mathbf{P},\ \mathbf{q}), \quad \tilde{G}(t) = \sum_{m=0}^{r} \frac{t^m}{m!} G_m(\mathbf{P},\ \mathbf{q}).$$

Upon substitution into the transformation equations (56) *two systems are obtained*

$$\frac{\partial G}{\partial q_n}(\mathbf{P},\ \mathbf{q}) = f_n(p_n,\ q_n), \quad \frac{\partial G}{\partial P_n}(\mathbf{P},\ \mathbf{q}) = g_n(P_n,\ Q_n) \tag{A.13}$$

and

$$\frac{\partial \tilde{G}}{\partial q_n}(\tilde{\mathbf{P}},\ \mathbf{q}) = f_n(p_n,\ q_n), \quad \frac{\partial \tilde{G}}{\partial \tilde{P}_n}(\tilde{\mathbf{P}},\ \mathbf{q}) = g_n(\tilde{P}_n,\ \tilde{Q}_n), \tag{A.14}$$

with respective solutions $(\mathbf{P}, \mathbf{Q})$ *and* $(\tilde{\mathbf{P}},\ \tilde{\mathbf{Q}})$. *Then,* (A.13) *and* (A.14) *can be solved uniquely for sufficiently small* t *so that*

$$(\tilde{\mathbf{P}},\ \tilde{\mathbf{Q}}) = (\mathbf{P},\ \mathbf{Q}) + \mathcal{O}(t^{r+t}). \tag{A.15}$$

Proof. Observe that $\tilde{G}(t) = G(t) + \mathcal{O}(t^{r+1})$ and therefore

$$\begin{aligned} f_n(p_n,\ q_n) &= \frac{\partial G}{\partial q_n}(\tilde{\mathbf{P}},\ \mathbf{q}) + \mathcal{O}(t^{r+1}) \\ g_n(\tilde{P}_n,\ \tilde{Q}_n) &= \frac{\partial G}{\partial P_n}(\tilde{\mathbf{P}},\ \mathbf{q}) + \mathcal{O}(t^{r+1}). \end{aligned} \tag{A.16}$$

From the second equation of (A.13) we calculate the derivative matrix

$$\boldsymbol{J}^{\mathbf{1}}(t) = \frac{\partial^2 G}{\partial \mathbf{P} \partial \mathbf{q}} = \left(\frac{\partial^2 G}{\partial P_n \partial q_m} \right) = \left(\sum_{j=1}^{N} \frac{\partial g_n}{\partial Q_j} \frac{\partial Q_j}{\partial q_m} \right).$$

Using the expansion $\mathbf{Q} = \mathbf{q} + \mathcal{O}(t)$ to calculate $\frac{\partial \mathbf{Q}}{\partial \mathbf{q}}$ and setting $t = 0$ yields

$$J^1_{n,m}(0) = \sum_{j=1}^{N} \frac{\partial g_n}{\partial Q_j}(\mathbf{P},\ \mathbf{Q})\delta_{j,m} = \frac{\partial g_n}{\partial q_m}(\mathbf{p},\ \mathbf{q}) = \delta_{m,n}\omega_n(p_n,\ q_n).$$

Since ω is nondegenerate at $(\mathbf{p}, \mathbf{q})$ by assumption, $\boldsymbol{J}^1(t)$ is nonsingular for $t = 0$ and for sufficiently small nonzero t the same holds by continuity. Since $\tilde{G}(t) = G(t) + \mathcal{O}(t^{r+1})$,

$$\tilde{\boldsymbol{J}}^1 = \frac{\partial^2 G}{\partial \tilde{\mathbf{P}} \partial \mathbf{q}}$$

is nonsingular for small t as well. Taking the smaller of the two values for t, we ensure that the first equtions of both systems (A.13) and (A.14) are solvable for $\mathbf{P}$. (Incidentally, this argument establishes that G and $\tilde{G}$ obtained by the technique in Section 4 are indeed generating functions of the second kind.) Next, we substitute the obtained $\mathbf{P}$ and $\tilde{\mathbf{P}}$ into the second equations of (A.13) and (A.14) and solve for $\mathbf{Q}$ and $\tilde{\mathbf{Q}}$, respectively. This is possible since the appropriate Jacobi matrix is

$$\boldsymbol{J}^2(t) = \left(\frac{\partial g_n}{\partial Q_m}(\mathbf{P},\ \mathbf{Q}) \right) = (\delta_{m,n}\omega_n(P_n,\ Q_n)),$$

and it is nondenerate for the chosen values of t by construction.

Having obtained $(\mathbf{P}, \mathbf{Q})$ and $(\tilde{\mathbf{P}},\ \tilde{\mathbf{Q}})$ we compare their Taylor expansions at $t = 0$. For that we differentiate equations (A.13) and (A.14) with respect to t to k-th order and solve for

$$\frac{d^k}{dt^k}(\mathbf{P},\ \mathbf{Q})|_{t=0} \quad \text{and} \quad \frac{d^k}{dt^k}(\tilde{\mathbf{P}}, \tilde{\mathbf{Q}})\big|_{t=0},$$

respectively. By virtue of (A.15), upon setting $t = 0$ the differentiated equations reduce to the same system as long as $k \le r$, and by nondegeneracy of $\boldsymbol{J}^1(0)$ and $\boldsymbol{J}^2(0)$ the solution is unique so that

$$\frac{d^k}{dt^k}(\mathbf{P},\ \mathbf{Q})|_{t=0} = \frac{d^k}{dt^k}(\tilde{\mathbf{P}},\ \tilde{\mathbf{Q}})|_{t=0}, \quad k = 0, \ldots, r$$

and therefore

$$(\mathbf{P},\ \mathbf{Q}) = (\tilde{\mathbf{P}},\ \tilde{\mathbf{Q}}) + \mathcal{O}(t^{r+1})$$

for all t as determined above.

ACKNOWLEDGMENT

This work was partially supported by the NSF, grant number DMS-9803567.

REFERENCES

1. M. J. Ablowitz and J. F. Ladik, A nonlinear difference scheme and inverse scattering, *Stud. Appl. Math.* **55**, 213 (1976).
2. M. J. Ablowitz, B. M. Herbst, and C. M. Schober, Numerical chaos, roundoff errors and homoclinic manifolds, *Phys. Rev. Lett.* **71**, 2683 (1993).
3. M. J. Ablowitz and C. M. Schober, Effective chaos in the nonlinear Schrödinger equation, *Contemporary Mathematics* **172**, 253 (1994).
4. M. J. Ablowitz, B. M. Herbst, and C. M. Schober, On the numerical solution of the sine-Gordon equation I. Integrable discretizations and homoclinic manifolds, *J. Comput. Phys.* **126**, 299 (1996).
   M. J. Ablowitz, B. M. Herbst, and C. M. Schober, On the numerical solution of the sine-Gordon equation II. Performance of numerical schemes, *J. Comput. Phys.* **131**, 354 (1997).
5. V. I. Arnold, *Mathematical Methods of Classical Mechanics* (Springer-Verlag, New York, 1978).
6. Th. J. Bridges, Multi-symplectic structures and wave propagation, *Math. Proc. Cambridge Philos. Soc.* **121**, 147 (1997).
7. Th. J. Bridges and S. Reich, *Multi-symplectic Integrators: Numerical Schemes for Hamiltonian PDEs that Conserve Symplectivity*, Internal Report, University of Surrey, U.K (1999).
8. P. J. Channell and C. Scovel, Symplectic integration of Hamiltonian systems, *Nonlinearity* **3**, 1 (1990).
9. K. B. Dysthe, Note on modification to the nonlinear Schrodinger equation for application to deep water waves, *Proc. Roy. Soc. Lond. A* **369**, 105 (1979).
10. B. Fornberg, *A Practical Guide to Pseudospectral Methods* (Cambridge Univ. Press, Cambridge, UK, 1998).
11. B. M. Herbst, F. Varadi, and M. J. Ablowitz, Symplectic methods for the nonlinear Schrödinger equation, *Math. Comput. Sim.* **37**, 353 (1994).
12. J. P. Holloway, On numerical methods for Hamiltonian PDEs and a collocation method for the Vlasov-Maxwell equations, *J. Comput. Phys.* **129**, 121 (1996).
13. A. Iserles, *Numerical Analysis of Differential Equations* (Cambridge Univ. Press, Cambridge, UK, 1996).
14. X. Lu and R. Schmid, Symplectic integration of sine-Gordon type systems, *Math. Comput. Sim.* **50**, 255 (1999).
15. J. E., Marsden, G. P. Patrick, and S. Shkoller, Multi-symplectic geometry, variational integrators, and nonlinear PDEs, *Comm. Math. Phys.* **199**, 351 (1999).
16. R. McLachlan, Symplectic integration of Hamiltonian wave equations, *Numerische Mathematik* **602**, 1 (1993).
17. R. McLachlan, On the numerical integration of ordinary differential equations by symmetric composition methods, *SIAM J. Sci. Comput.* **16**, 151 (1995).

18. D. W. McLaughlin and C. M. Schober, Chaotic and homoclinic behavior for numerical discretizations of the nonlinear Schrödinger equation, *Physica D* **57**, 447 (1992).
19. P. D. Miller, *Macroscopic Lattice Dynamics*, Ph.D. thesis (University of Arizona, 1994).
20. S. Reich, Multi-symplectic Runge–Kutta collocation methods for Hamiltonian wave equations, *J. Comput. Phys.* **157**, 473 (2000).
21. J. M. Sanz-Serna and M. P. Calvo, *Numerical Hamiltonian Problems* (Chapman & Hall, London, 1994).
22. C. M. Schober, Symplectic integrators for the Ablowitz–Ladik discrete nonlinear Schrödinger equation, *Phys. Lett. A* **259**, 140 (1999).
23. A. G. Shagalov, Symplectic Integrators for Wave Equations, *Int. J. Mod. Phys. C* **10**, 1 (1999).
24. Y. F. Tang, V. M. Pérez-García, and L. Vázquez, Symplectic methods for the Ablowitz–Ladik Model, *Appl. Math. Comput.* **82**, 17 (1997).
25. V. E. Zakharov and A. B. Shabat, Exact theory of two-dimensional self-focusing and one-dimensional self-modulation of waves in nonlinear media. *Soviet Phys. Jetp.* **34**, 62 (1972).